CHAPTER 4

Effects of Thermal Ageing on Microstructural Evolution for JLF-1 and CLAM Steels

In this chapter, the effects of thermal ageing on microstructural evolution will be reported and discussed.

4.1 Introduction

The RAFM steels are the tempered martensitic steels. The formation processes are schematically demonstrated in *Fig.4-1*.

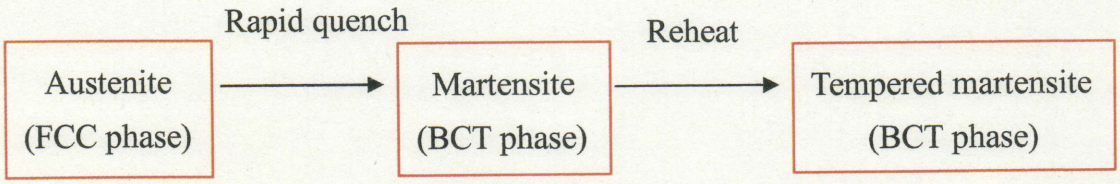

Fig. 4-1 Typical phase transformation processes for RAFM steels

When the steel is heated to the temperature much higher than that austenitic phase is formed, the solid solution is produced in an FCC phase. During this stage, full dissolution of all elements is expected. After quenching with vary fast cooling rate, the austenitic phase is transformed into martensitic phase, which has a supersaturated carbon atom concentration and BCT phase.

Since martensite is too hard and brittle for actual application, the tempering treatment is necessary. After tempering, the tempered martensite with BCT phase is formed accompanied the recovery of ductility and the decrease in hardness. During this tempering stage, carbide and nitride particles form on prior austenite grain boundary, ferrite subgrain and lath boundary. When steel is put into service at temperature below the final tempering temperature, further precipitation of particles may occur.

Therefore, the typical microstructure of RAFM steels consists of full-tempered martensitic structure with high density dislocations and various types of precipitates.

The schematic illustration of the microstructural characteristics for typical RAFM steels is shown in *Fig. 4-2*, and the formation processes of martensitic lath are demonstrated in *Fig. 4-3*.

Generally, the microstructure parameters to affect the mechanical properties include: grain and grain boundary, lath and lath boundary, precipitates, dislocations, and so on. The fine boundaries and precipitates will act as the strong obstacles to impede the dislocations motion in steel. The detailed microstructural characteristics before and after ageing will be introduced in next section.

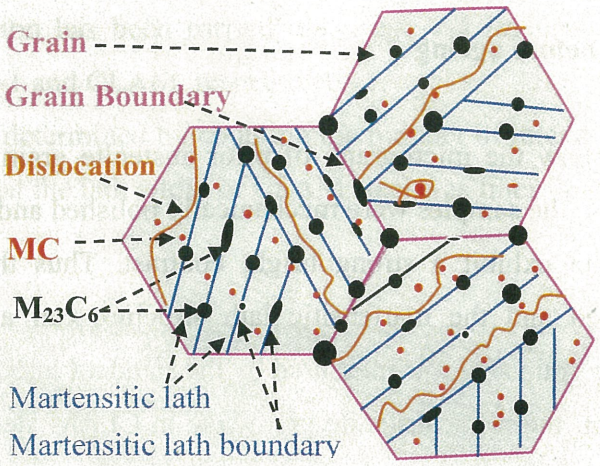

Fig. 4-2 Schematic illustration of microstructural characteristic for RAFM steels

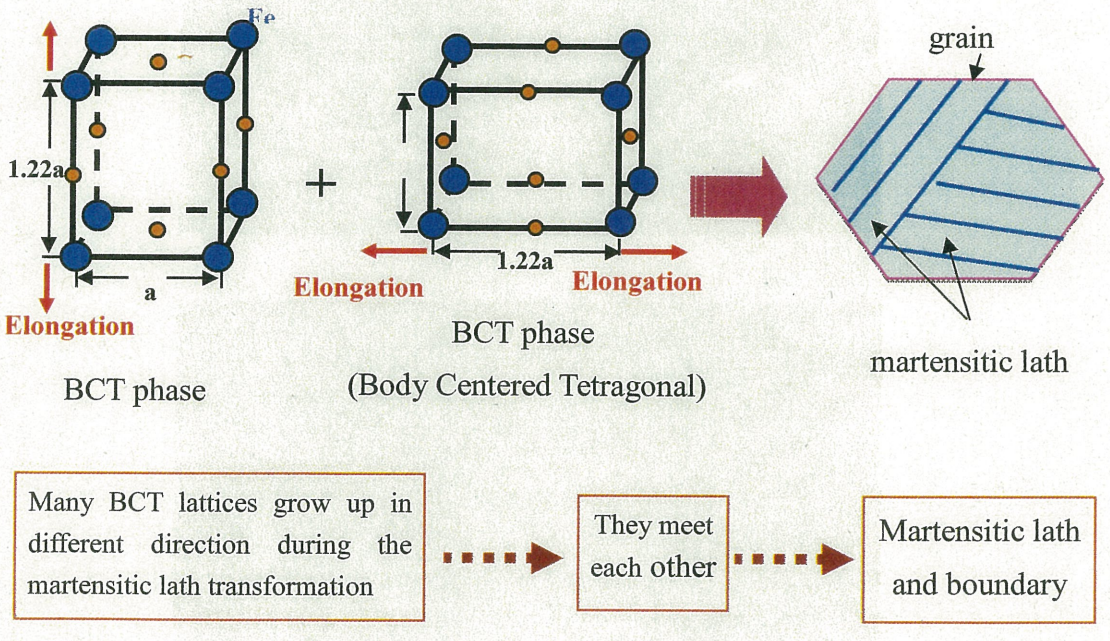

Fig.4-3 Schematic showing the formation processes of martensitic lath

4.2 Microstructure observation before ageing

4.2.1 Prior austenite grain before ageing

Figs. *4-4 (a)* and *(b)* show the micrograph of prior austenite grain by SEM for JLF-1 and CLAM, respectively. Because the samples were mechanically polished and then etched by chemical solution, the precipitates can exhibit a strong bright contrast. Thus the prior austenitic grain boundary can be determined and the martensitic lath structure can also be observed by the precipitates distribution. The grain size was measured by the standard intersection count method.

These figures show that, the prior austenite grain size in CLAM steel was obviously smaller than that in JLF-1 steel.

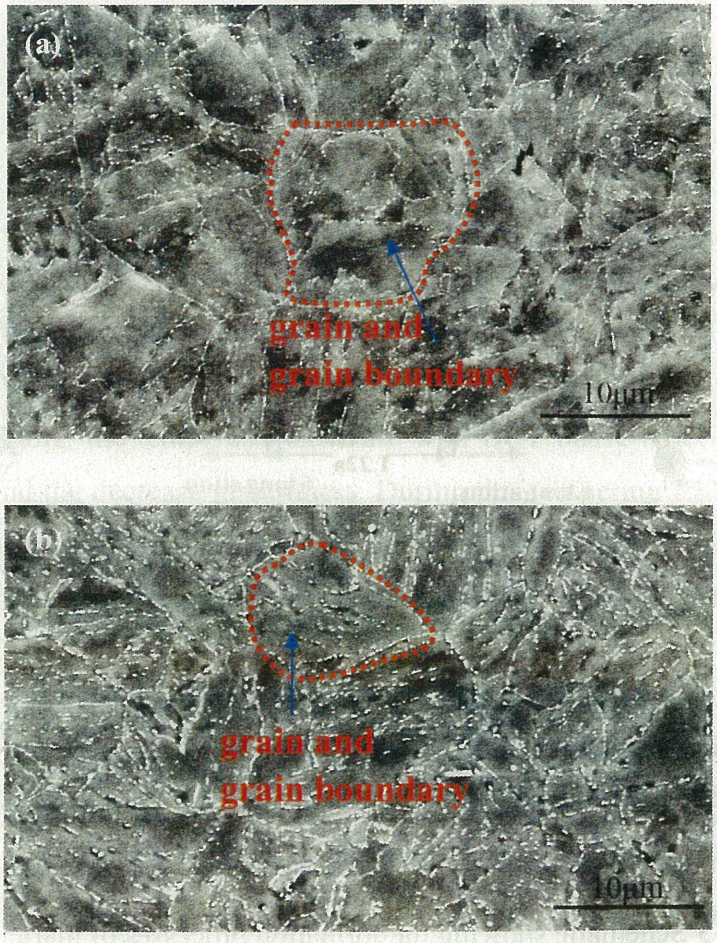

Fig. 4-4 Micrograph showing an overview of austenitic grains and precipitates distribution in the before ageing condition: (a) JLF-1 and (b) CLAM.

4.2.2 Martensitic lath before ageing

The TEM observation has been carried out. Figs. *4-5 (a) and (b)* show the micrograph of martensitic laths for JLF-1 and CLAM, respectively.

The lath width was determined by counting the number of intersections of lath boundaries and straight lines. It seems that the lath width of CLAM steel was finer than that of JLF-1.

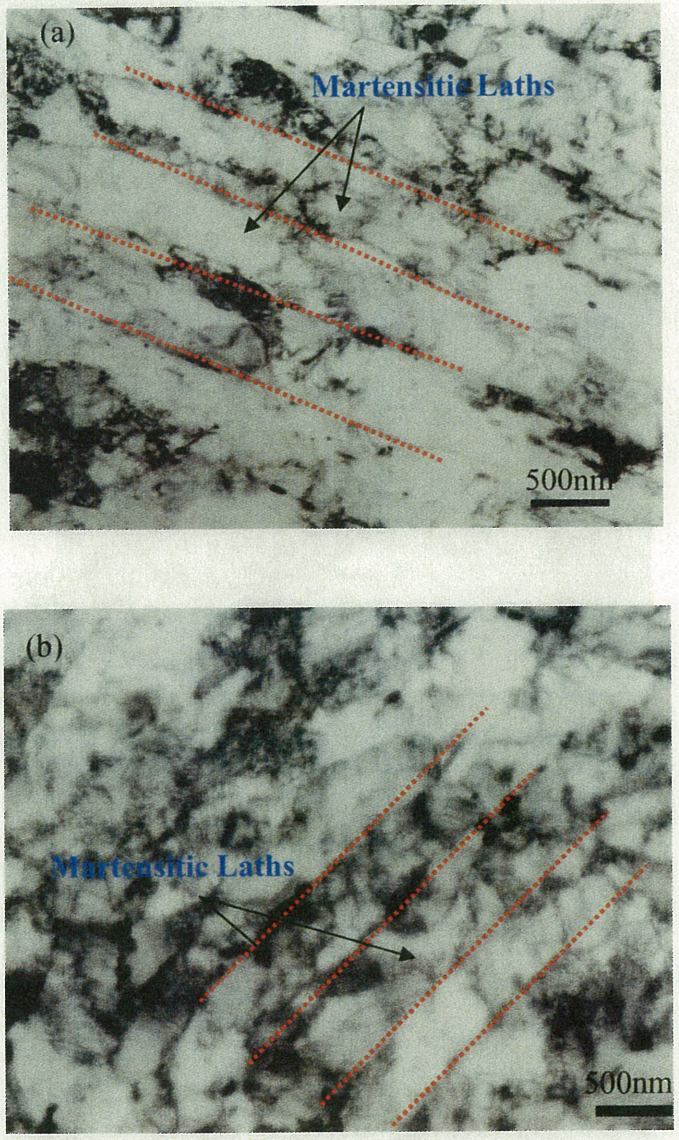

Fig. 4-5 Micrographs of martensitic laths before ageing: (a) JLF-1 and (b) CLAM

4.2.3 Precipitates before ageing

The micrographs for the precipitates before ageing are shown in *Figs. 4-6 (a)* and *(b)* for JLF-1 and CLAM, respectively.

There were two types of precipitates: $M_{23}C_6$ and MC. The $M_{23}C_6$ precipitates usually were distributed in the grains and lath boundaries, while fine globular MC particles were formed mainly at matrix. It seems that there is no significant difference in the shape and size of the precipitates for the both steels.

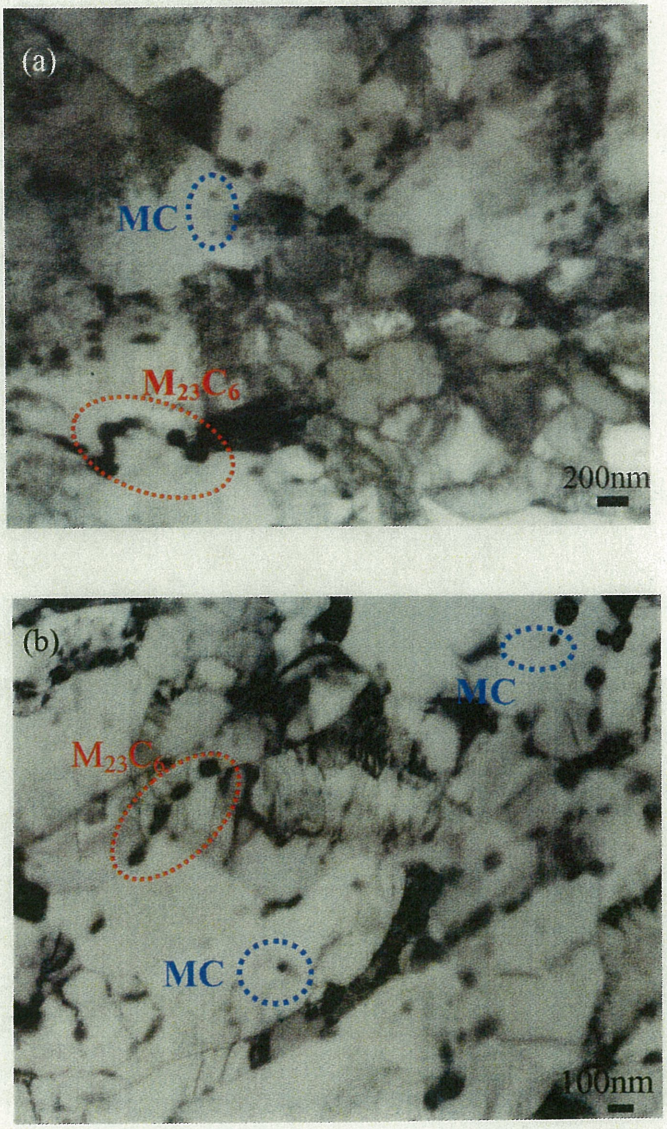

Fig. 4-6 Micrographs of the precipitates before ageing for: (a) JLF-1 and (b) CLAM

4.2.4 Dislocations before ageing

There are dense dislocations interior of the grains and mastensitic laths. The micrographs of dislocations and dislocation networks are shown in *Figs. 4-7 (a)* and *(b)* for JLF-1 and CLAM, respectively.

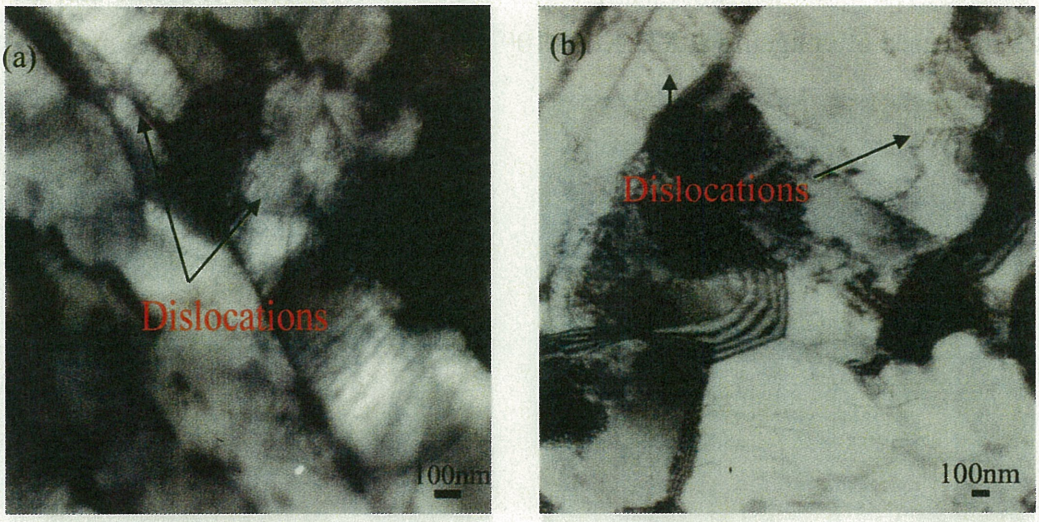

Fig. 4-7 Micrographs of dislocation structure before ageing for: (a) JLF-1 and (b) CLAM.

4.2.5 Summary of microstructural parameters before ageing

Some important microstructure parameters were measured and analyzed for CLAM and JLF-1 steels before ageing, and the results are summarized in *Table 4-1*. Obviously, CLAM has finer grain size, smaller lath width and almost same average size of carbide than those of JLF-1.

Table 4-1 The microstructural parameters for JLF-1 and CLAM steels before ageing

	JLF-1 [67]	CLAM
Prior austenite grain size, /μm	10.0	6.0
Lath width, /μm	0.50	0.44
Carbide size, /nm	104	104

4.3 Microstructural evolution after ageing for 100 h

4.3.1 Microstructural evolution after ageing at 823 K for 100 h

The microstructural evolution after ageing at 823 K for 100 h was examined. The TEM micrographs are shown in *Figs. 4-8* and *4-9* for JLF-1 and CLAM, respectively.

After ageing, the microstructure is similar to that before ageing, which is composed of tempered-martensitic structure with dense precipitates and dislocations. It seems that the density of precipitates increased after ageing at 823 K for 100 h, compared with that before ageing.

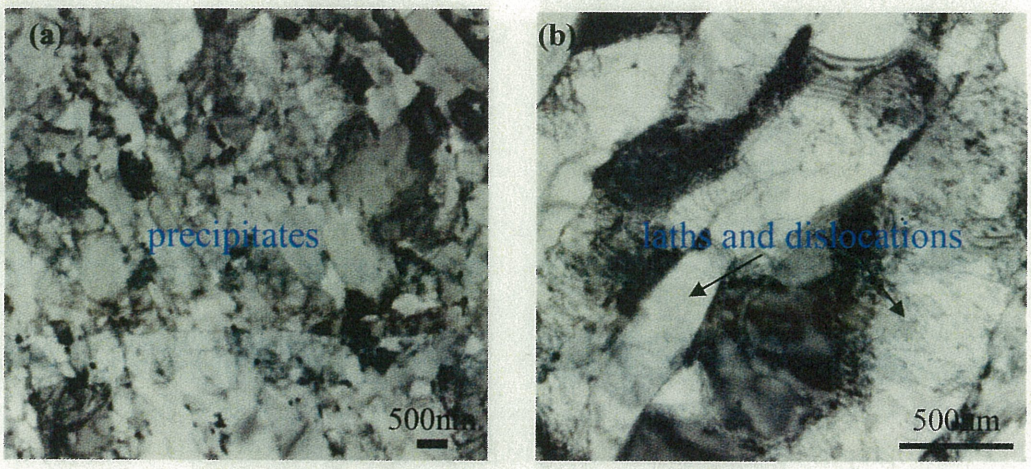

Fig. 4-8 TEM micrographs for JLF-1 after ageing at **823 K for 100 h**:
(a) precipitates and (b) martensitic laths with high density of dislocations

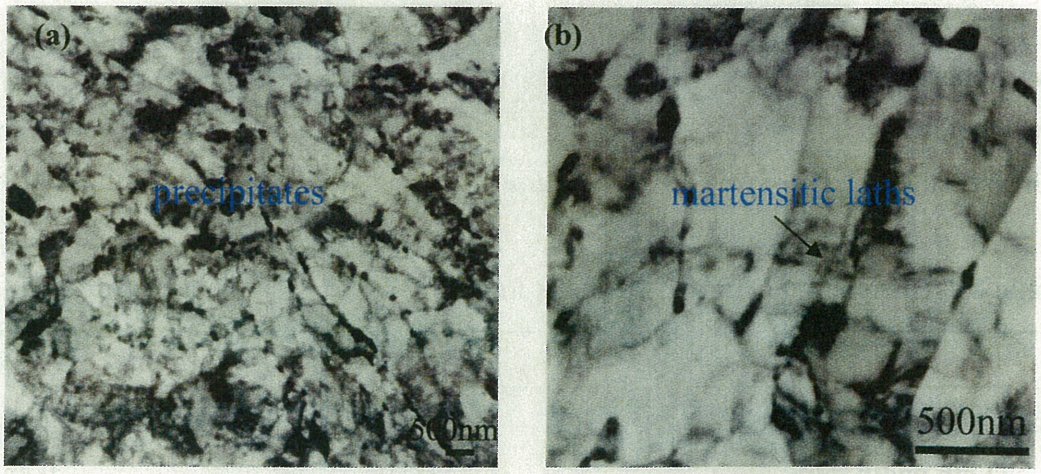

Fig. 4-9 TEM micrographs for CLAM after ageing at **823 K for 100 h**:
(a) precipitates and (b) martensitic laths

4.3.2 Microstructural evolution after ageing at 923 K for 100 h

The microstructure evolutions after ageing at 923 K for 100 h are shown in *Figs. 4-10* and *4-11*, for JLF-1 and CLAM, respectively.

After ageing at 923 K for 100 h, the quantity of precipitates continued to increase, compared with that before ageing. However, the partial recovery of lath structure and dislocations can also be observed.

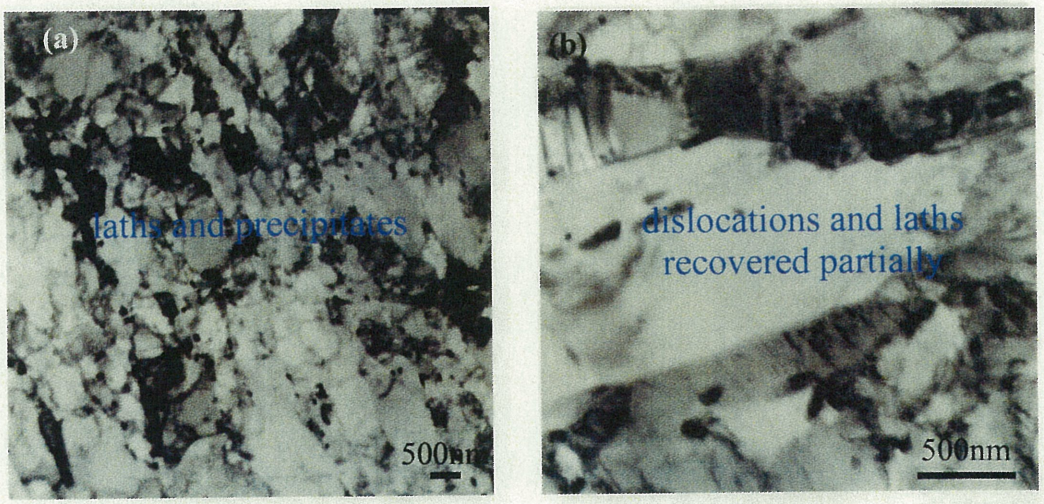

Fig. 4-10 TEM micrographs for JLF-1 after ageing at **923 K for 100 h**:
(a) laths and precipitates and (b) partial recovery of laths and dislocations

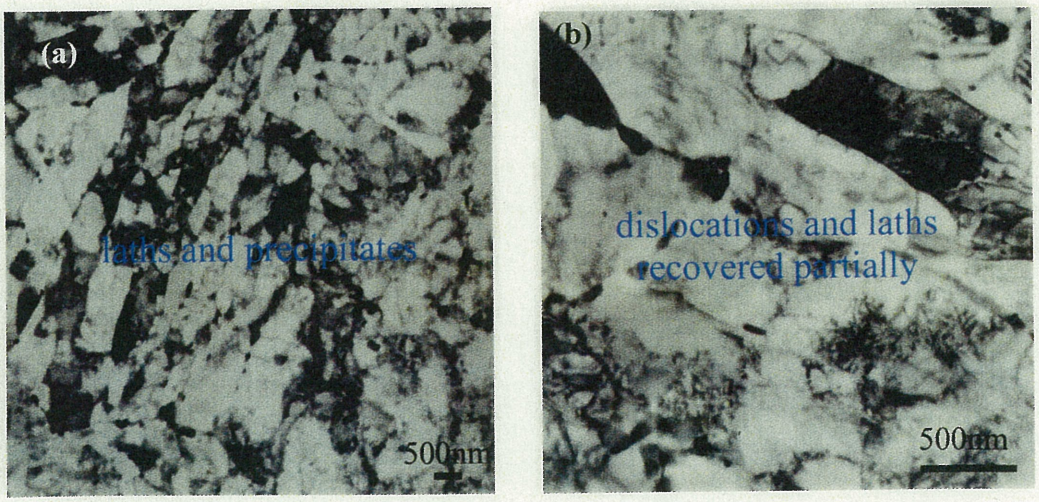

Fig. 4-11 TEM micrographs for CLAM after ageing at **923 K for 100 h**:
(a) laths and precipitates and (b) partial recovery of laths and dislocations

4.3.3 Microstructural evolution after ageing at 973 K for 100 h

The microstructural evolutions after ageing at 973 K for 100 h are shown in *Fig. 4-12* and *4-13*, for JLF-1 and CLAM, respectively.

After ageing at 973 K for 100 h, it is obvious that the amount of precipitates decreased, compared with that before ageing. In addition, the recovery of laths and dislocations were also enhanced.

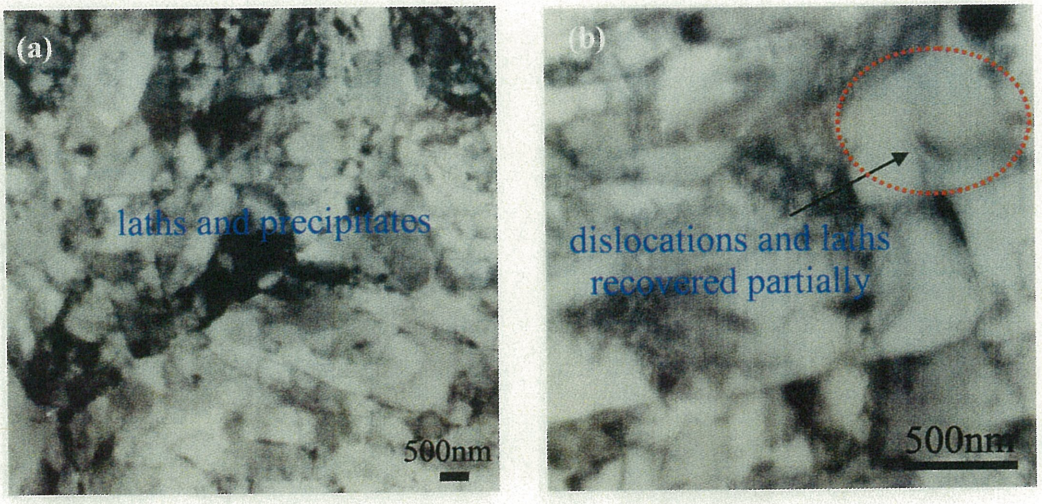

Fig. 4-12 TEM micrographs for JLF-1 after ageing at **973 K for 100 h**:
(a) laths and precipitates and (b) partial recovery of laths and dislocations

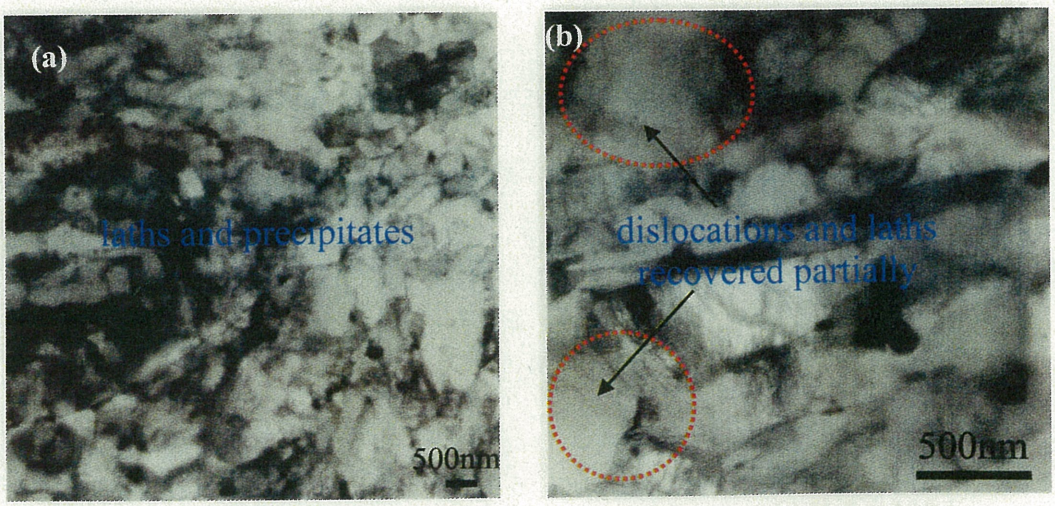

Fig. 4-13 TEM micrographs for CLAM after ageing at **973 K for 100 h**:
(a) laths and precipitates and (b) partial recovery of laths and dislocations

4.4 Microstructural evolution after ageing for 2000 h

4.4.1 Microstructural evolution after ageing at 823 K for 2000 h

The microstructural evolution after ageing at 823 K for 2000 h was observed. The micrographs are shown in *Figs. 4-14* and *4-15* for JLF-1 and CLAM, respectively.

Clearly, the density of precipitates increased remarkably after ageing at 823 K for 2000 h for the both steels, compared with that before ageing. No significant recovery of martensitic laths and dislocations was detected.

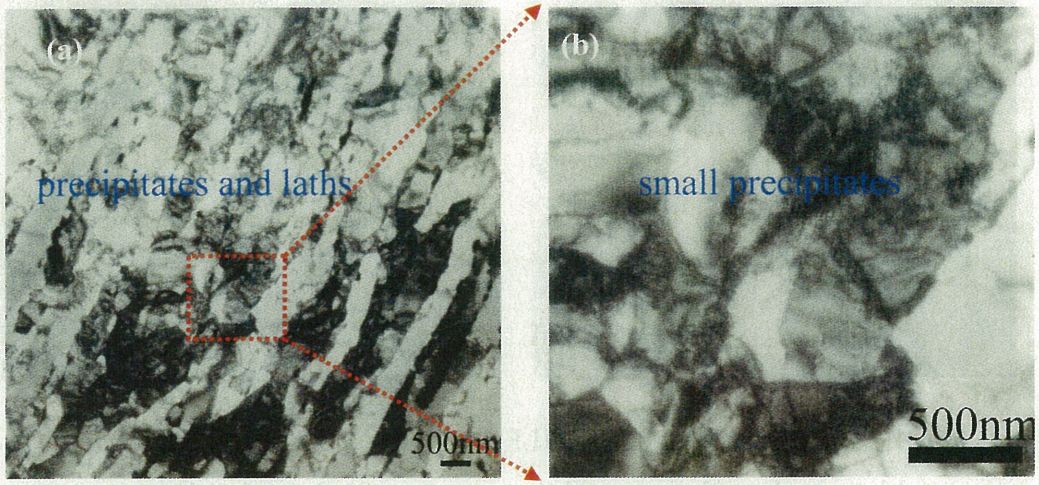

Fig. 4-14 TEM micrographs for JLF-1 after ageing at **823 K for 2000 h**:
(a) precipitates and laths, (b) small precipitates in high magnification

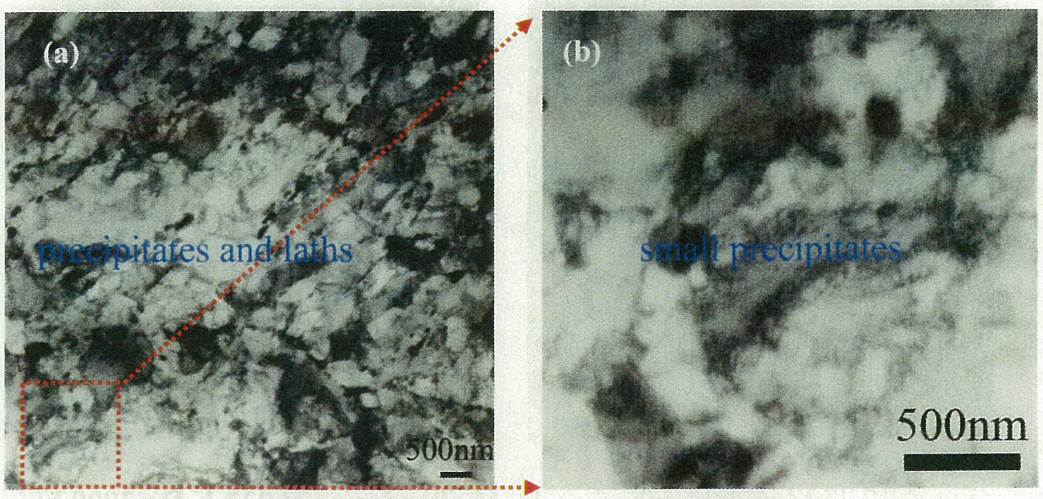

Fig. 4-15 TEM micrographs for CLAM after ageing at **823 K for 2000 h**:
(a) precipitates and laths, (b) small precipitates in high magnification

4.4.2 Microstructural evolution after ageing at 923 K for 2000 h

The microstructural evolution after ageing at 923 K for 2000 h was observed and the micrographs are shown in *Figs. 4-16* and *4-17* for JLF-1 and CLAM, respectively.

After ageing at 923 K for 2000 h, the quantity of precipitates was also increased. At the same time, the slight recovery of laths and dislocations took place.

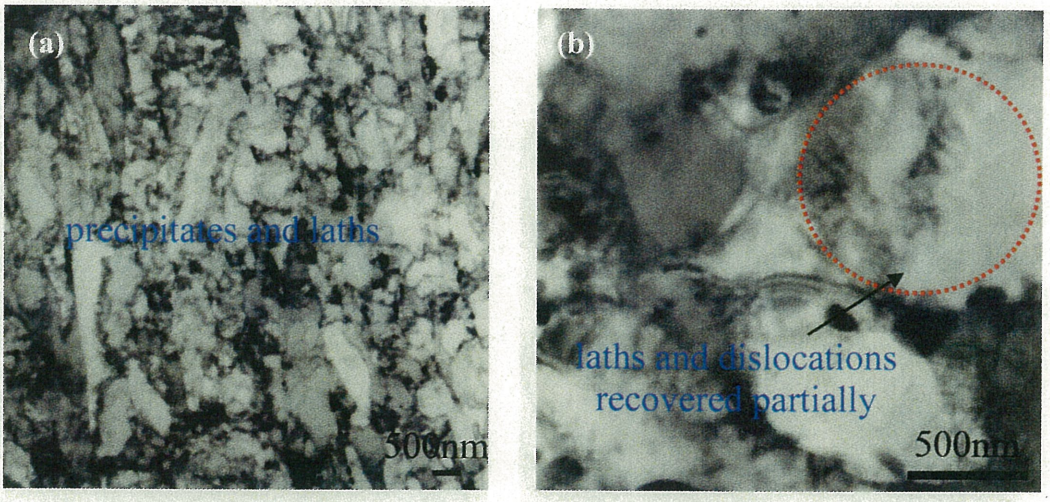

Fig. 4-16 TEM micrographs for JLF-1 after ageing at **923 K for 2000 h**:
(a) laths and precipitates and (b) recovery of laths and dislocations

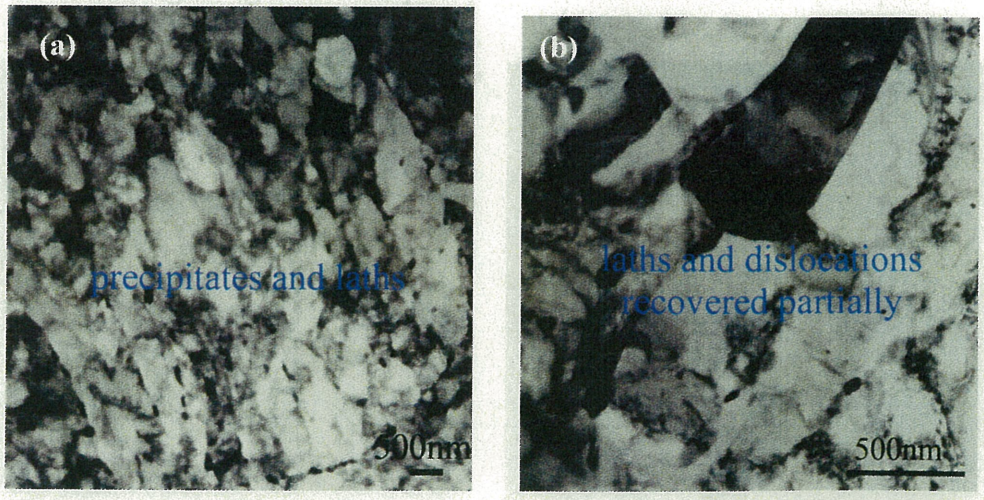

Fig. 4-17 TEM micrographs for CLAM after ageing at **923 K for 2000 h**:
(a) laths and precipitates and (b) recovery of laths and dislocations

4.5 Total number density of precipitates

The total number density of precipitates before and after ageing was analyzed. The results are shown in *Figs. 4-18* and *4-19* for ageing time of 100 and 2000 h, respectively.

After ageing at 823 and 923 K for 100 h, the Fig. 4-18 showed that, the total number density of precipitates increased for the both steels, compared with that before ageing. However, the total density decreased after ageing at 973 K for 100 h.

After ageing up to 2000 h, as shown in Fig. 4-19, the total density of precipitates further increased. In addition, they increased with the increasing temperature from 823 to 923 K.

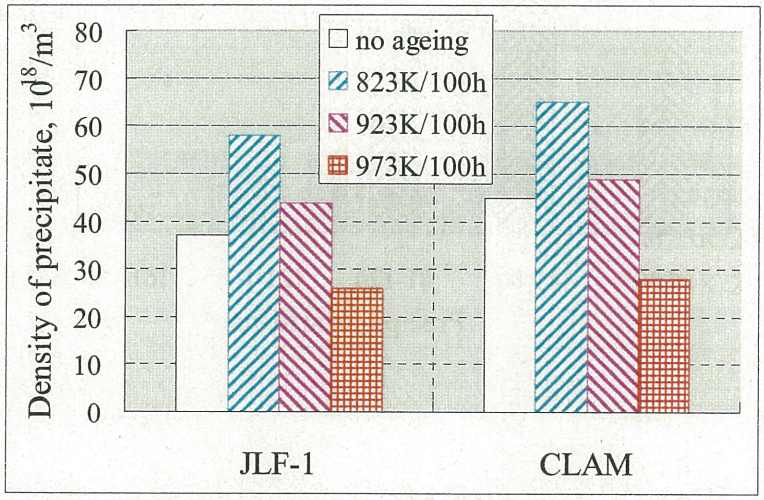

Fig. 4-18 Total number density of precipitates after ageing for 100 h for JLF-1 and CLAM

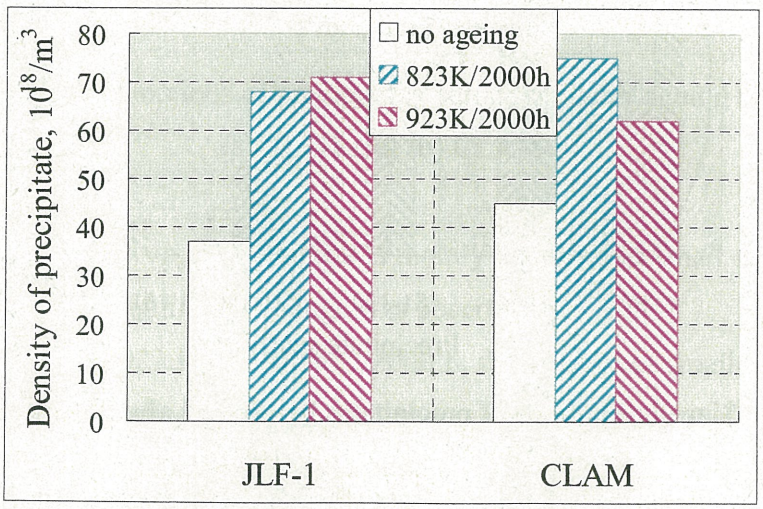

Fig. 4-19 Total number density of precipitates after ageing for 2000 h for JLF-1 and CLAM

4.6 Size distribution of precipitates

The size distribution of precipitates was analyzed before and after ageing. The results are shown in *Figs. 4-20* and 4-*21* for ageing time of 100 and 2000 h, respectively.

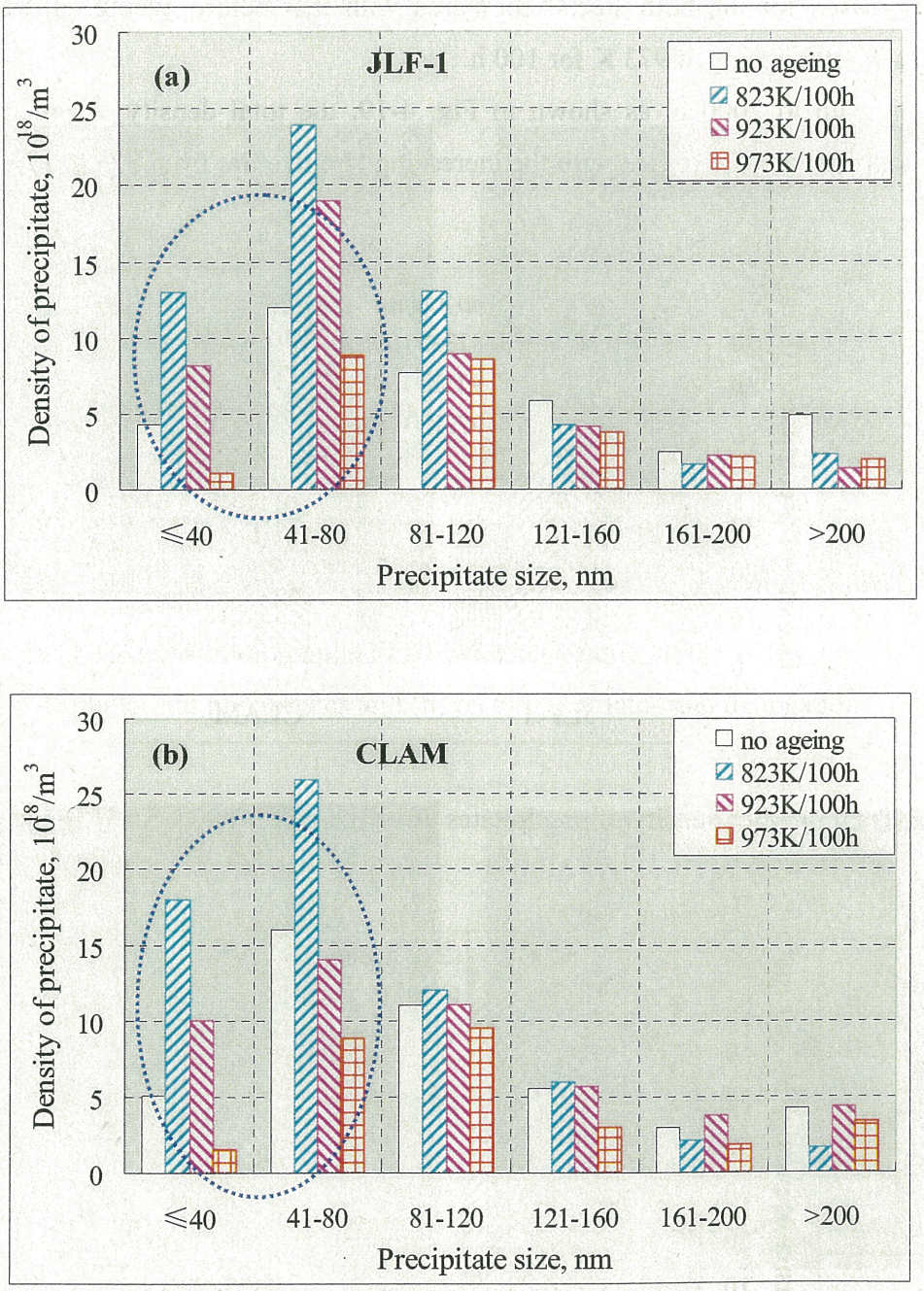

Fig. 4-20 Size distributions of precipitates before and after ageing for **100 h**:
(a) JLF-1 and (b) CLAM

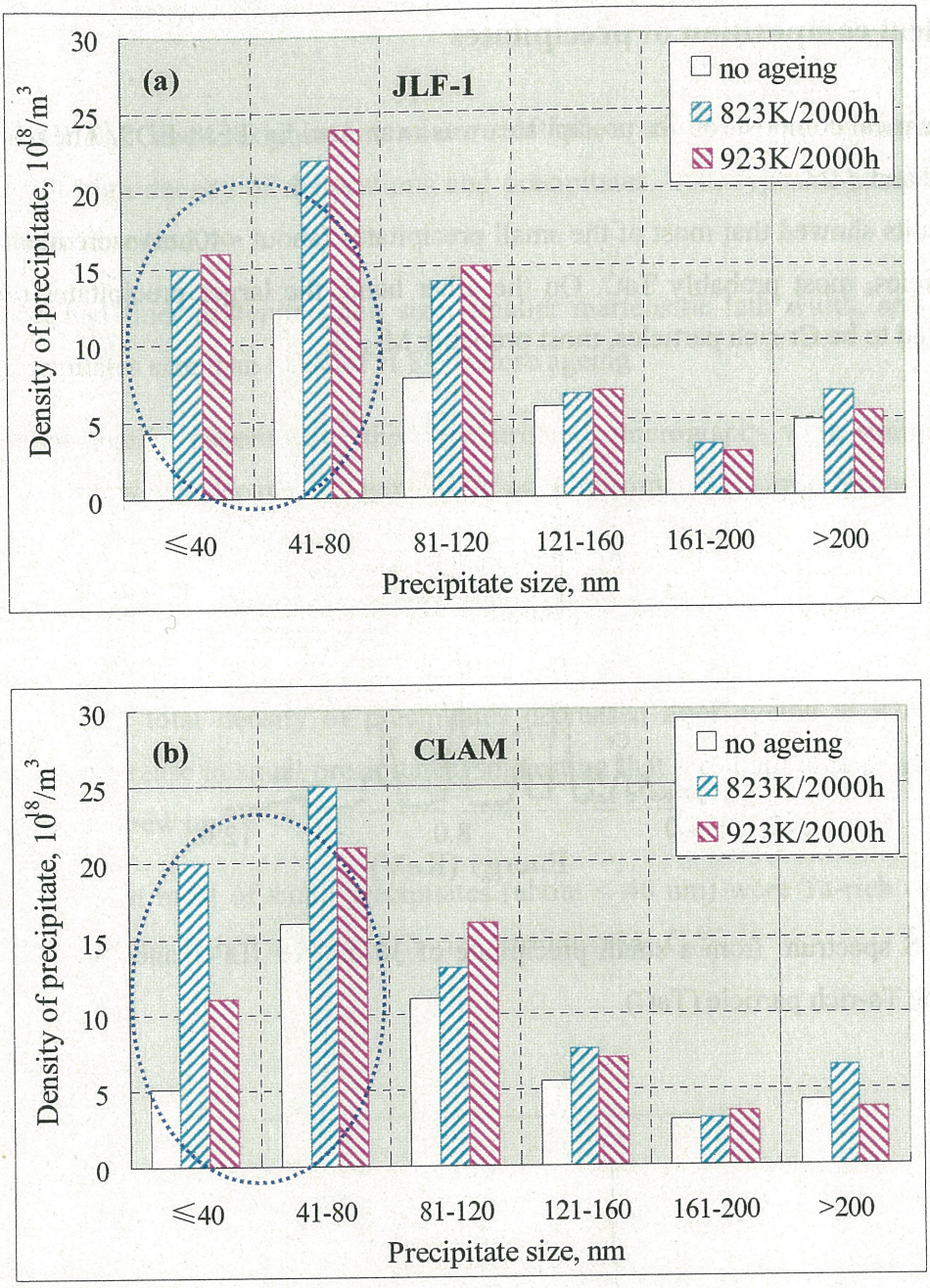

Fig. 4-21 Size distributions of precipitates before and after ageing for **2000 h**:
(a) JLF-1 and (b) CLAM

The remarkable change in size distribution is mainly localized in small size regions (<80 nm). At the larger size regions, no significant change was observed.

After ageing at 823 and 923 K for 100 and 2000 h, the density of small precipitates (<80 nm) increased for the both steels, indicating small precipitates were newly formed. However, the density of small precipitates decreased remarkably after ageing at 973 K for 100 h, suggesting the small precipitates disappeared by dissolution or grew up.

4.7 Chemical composition of precipitates

The chemical composition for precipitates was examined by TEM-EDS. The results are shown in *Figs. 4-22* and *4-23*.

The results showed that most of the small precipitates (about <40nm) were identified to be the Ta-rich particles, most probably TaC. On the other hand, the larger precipitates (about 120 nm) were identified to be Cr-rich particles, most probably $M_{23}C_6$.

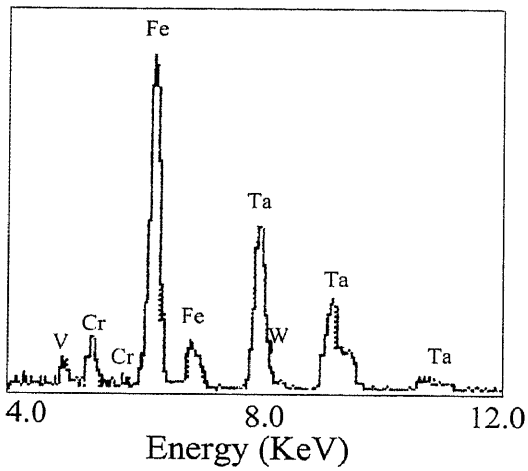

Fig. 4-22 EDS spectrum from a small precipitate of 30 nm for JLF-1 aged at 823 K for 2000 h, identifying the Ta-rich particle (TaC).

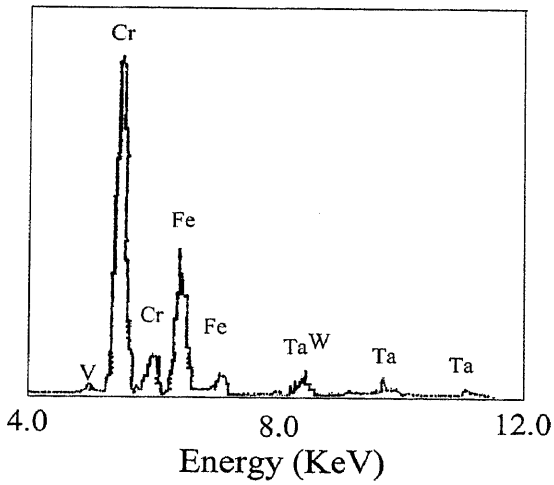

Fig. 4-23 EDS spectrum from a larger precipitate of 120 nm for JLF-1 aged at 823 K for 2000 h, identifying Cr-rich particle ($M_{23}C_6$).

4.8 Summary

1. JLF-1 and CLAM steels exhibited a mixture of lath-martensitic and tempered-martensitic structure with high density of dislocations and precipitates. Two types of precipitates, $M_{23}C_6$ and TaC, were observed.

2. CLAM steel had finer austenite grain size, smaller martensitic lath width, and almost same average precipitates size than those of JLF-1 before ageing.

3. After different ageing experiments, the microstructure micrographs were similar to those of before ageing. However, the partial recovery for aged specimens occurred for the both steels.

4. The analysis of microstructure with TEM showed that, the total density of precipitates increased after ageing at 823 and 923 K for 100 and 2000 h, mostly because of the increase in number density of small precipitates (<80 nm), indicating that small precipitates were newly formed. However, total density of precipitates decreased after ageing at 973 K for 100 h because of the decrease in small precipitates, suggesting that the small precipitates disappeared by dissolution or grew up.

5. EDS identified that most of small precipitates (about < 40 nm) were Ta-rich carbides (TaC), and larger precipitates (~120 nm) were Cr-rich carbides ($M_{23}C_6$).

CHAPTER 5

Discussion and Analysis

In this study, the effects of thermal ageing on mechanical properties and microstructure were examined for JLF-1 and CLAM steels. In this chapter, the relation between the mechanical properties and microstructural evolution will be investigated, and the possible mechanisms will be discussed.

5.1 The dispersed obstacle model

After thermal ageing, the microstructural evolution may occur, which will lead to the possible change in mechanical property. The correlation between them should be investigated to clarify the mechanism.

A traditional disperse obstacle model can be used to predict theoretically the relation between the hardness change and microstructure [98], which was already applied in many radiation hardening materials successfully [99-100].

This model involves the interaction forces of various defects as they impede dislocation motion along the slip plane [98]. This model is generally derived from Orowan's theory. For slip to occur, the dislocation must either move around the defects or through the defects. If the defect, such as the particle, is very strong, the dislocation can not shear it and move through easily. Thus, the dislocation bends between the particles, leaving a dislocation ring about each particle. In the case, energy must be supplied to increase the total length of dislocation line, and the basic stress is required. The process can be schematically illustrated in *Fig. 5-1*.

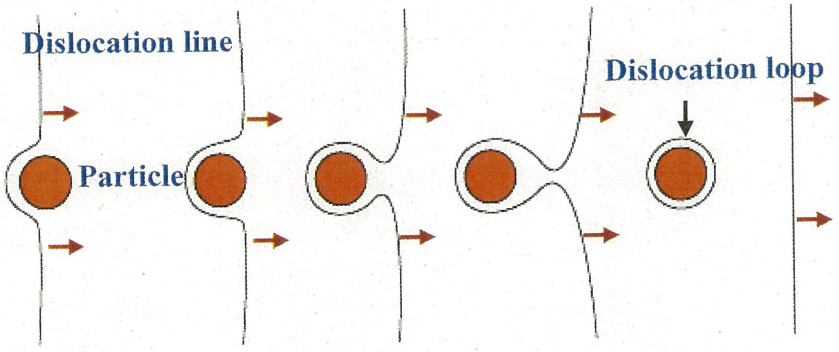

Fig. 5-1 Dislocation moves along a slip plane and passes by the particle (Orowan theory)[88]

Based on the model, the following equation can be used to correlate the hardness and microstructure change [101]:

$$\Delta HV = C_1 \times M \times \alpha \times G \times b \times \Delta(N_i D_i)^{1/2} \qquad (5\text{-}1)$$

where ΔHV = change in hardness,

C_1 = 3 (an empirical relation between the hardness and yield stress),

M = Taylor factor (3.06),

α = a parameter that describes the strength of the barrier (assumed 1.0 for carbide),

G = shear modulus (about 80 GPa for RAFM steels),

b = Burgers vector magnitude (0.268 nm),

N_i = number density of defects of a given type,

D_i = diameter of defects of a given type.

In irradiation condition, a lot of different defects will be formed, such as vacancy, void, bubble, precipitates, dislocation, and so on [99]. Different from that, in the present ageing conditions, the contribution of dislocations and other defect clusters to hardening was assumed small and neglected. The dominant obstacles against the deformation were assumed to be the precipitates only. And the parameter of barrier strength (α) equaled to 1.0 was usually expected for the strong particle.

In this calculation, two typical ageing conditions, hardening condition (823K/2000h) and softening condition (973K/100h) were chosen. *Figs. 5-2* and *5-3* show the calculated hardness change produced by precipitates change for JLF-1 and CLAM, respectively. For comparison, the measured hardness values are also listed.

The results show that, after ageing at 823 K for 2000 h, the calculated hardness change almost agreed with the measured ones for the both steels. Thus, it can be considered that the hardness change in this ageing condition was mainly due to the change in precipitates.

However, as indicated in the figures, there is a large difference between the measured and calculated data after ageing at 973 K for 100 h. It is obvious that the change in the precipitates alone cannot account for the change in hardness, indicating that some other factors will also operate.

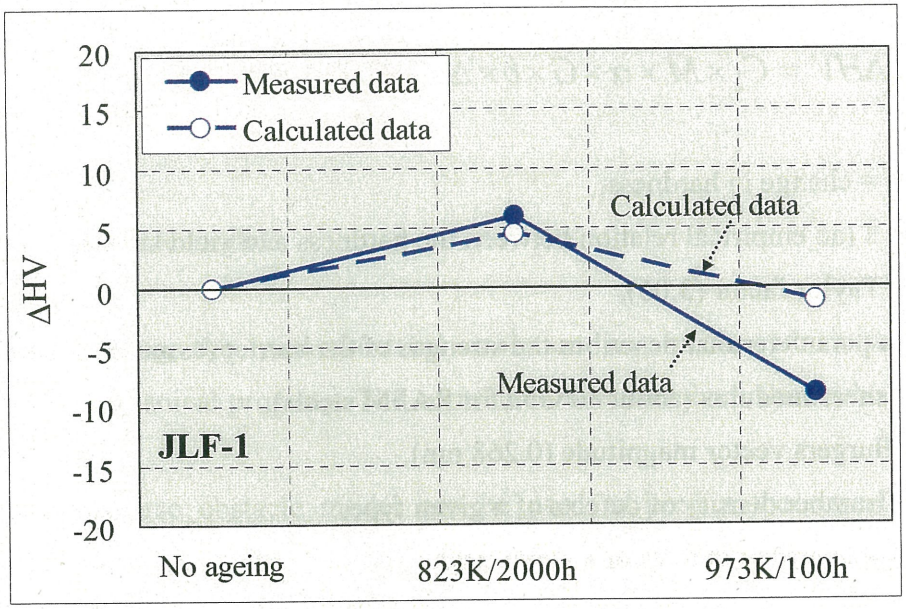

Fig. 5-2 The calculated hardness change by dispersed obstacle model for JLF-1 steel after thermal ageing conditions: 823K/2000h and 973K/100h, compared with the measured values.

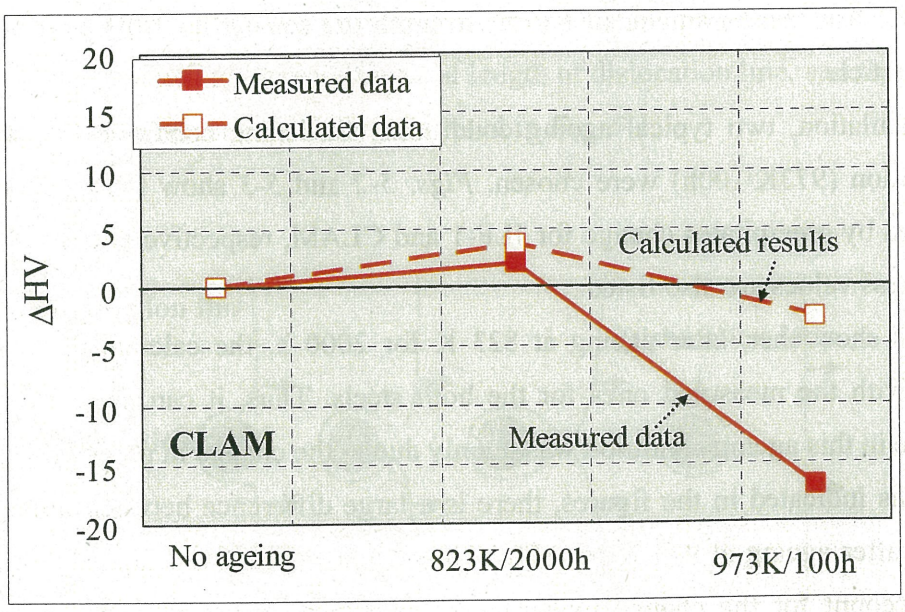

Fig. 5-3 The calculated hardness change by dispersed obstacle model for CLAM steel after thermal ageing conditions: 823K/2000h and 973K/100h, compared with the measured values.

5.2 Thermal activation analysis

The present experiments and analysis showed that the typical hardening took place by ageing at 823 K, and softening occurred by ageing at 973 K. In this section, correlation of the hardness data is attempted based on the thermal activation process.

In this analysis, ageing is assumed to be induced by migration of the constituent species (most probably carbon) with activation energy of E_m. The jump frequency of the species during the ageing is given by modified Arrhenius equation [102]:

$$\upsilon = \upsilon_0 \times \exp(-E_m / kT) \qquad (5\text{-}2)$$

where

υ_0 = thermal vibration frequency, 10^{13}/s

E_m = migration energy, eV

κ = Boltzsman energy, 0.8625 X 10^{-4} ev/K

T = absolute temperature, K

Thus,

$$\text{Total jumps during the ageing} = \upsilon \times t_a \qquad (5\text{-}3)$$

where t_a is the ageing time, s.

Figs. *5-4* and *5-5* show the hardness changes against the total number of jumps for different ageing conditions, assuming the migration energy of 1.6, 2.0 and 2.4 eV for JLF-1 and CLAM, respectively.

Usually the migration energy for carbon in martensitic phase varies in a range of 1.0 to 2.7 eV from the literature [103-104]. In this equation, the typical energy values of 1.6, 2.0 and 2.4 were chosen for calculation.

As shown in the figures, the total number of jumps was not an appropriate correlation parameter in any case of the activation energy. This means that the hardness change by ageing was not thermally activated process with the particular activation energy.

The results also showed that, by the ageing at 873 to 923 K, the hardness was almost independent from the ageing time.

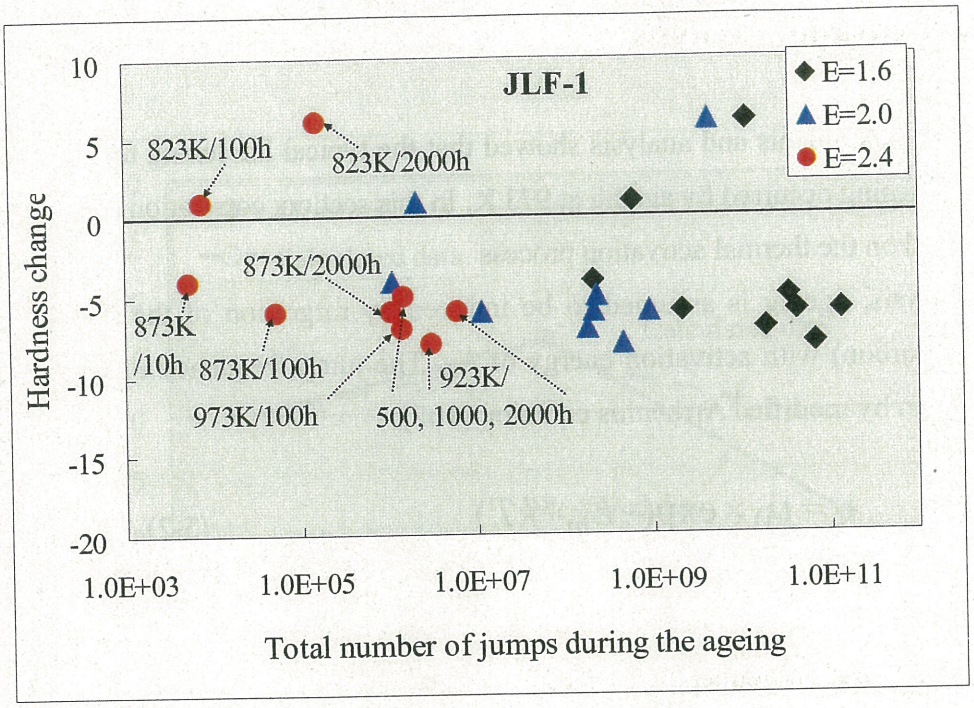

Fig. 5-4 Hardness change versus total number of jumps in different ageing conditions for JLF-1 steel (the migration energy E was assumed to be 1.6, 2.0 and 2.4 eV).

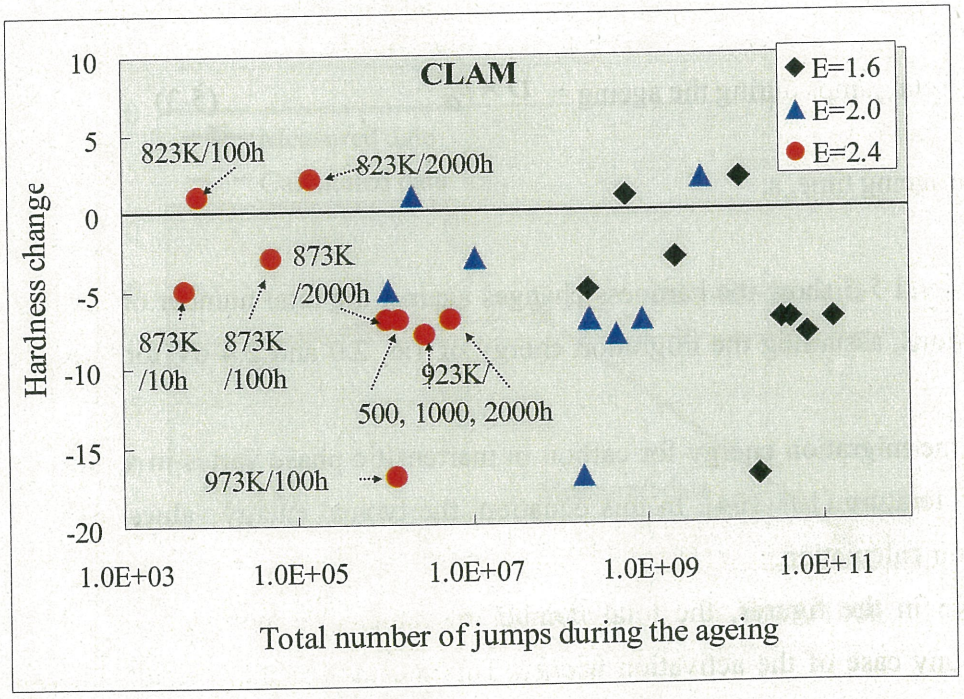

Fig. 5-5 Hardness change versus total number of jumps in different ageing conditions for CLAM steel (the migration energy E was assumed to be 1.6, 2.0 and 2.4 eV).

5.3 Precipitates behavior

5.3.1 Introduction

Precipitates play the very important role in RAFM steels. The typical precipitates in the ferritic steels are summarized in *Table 5-1*.

Table 5-1 The most common precipitates in typical 8-12% Cr steel [105]

Precipitate	Formula	Remark
$M_{23}C_6$	$(Cr, Fe, Mo)_{23}C_6$	Precipitates during tempering
MX	(Nb, Ta, V)(N, C)	Precipitate during tempering
M_6C	$(Fe_3 (W, Mo)_3)C$ $(Fe_4(W, Mo)_2)C$	Precipitated during long-term ageing, creep and irradiation
Laves phase	$(Fe, Cr)_2(Mo, W)$	Precipitated during long-term ageing, creep and irradiation

The $M_{23}C_6$ is the common precipitate in the steel, usually formed in grain and lath boundaries, and with a spherical or thin plate shape. The coarsening of $M_{23}C_6$ particles can be enhanced by long-term ageing and/or creep deformation.

The spherical MX is another important precipitate with a small size, distributed uniformly in matrix and in sub-boundaries. Usually, in RAFM steels containing Ta and low level of N, MX refers to (Ta,V)C.

M_6C are only formed during long-term creep or ageing processes at relatively high temperature. It is an undesired brittle phase. The formation of M_6C is reported to be done by consuming the MX particles [106].

Laves phase is another undesired inter-metallic compound. It is not present after tempering, but precipitates on grain boundaries and sub-boundaries during long-term creep, thermal ageing and irradiation. Similar to the M_6C phase, Laves phase is a brittle phase and can lead to the deterioration of creep properties. With the increase in W content, the possibility for precipitation of Laves phase will increase.

The possible precipitate processes of RAFM steels during the blanket service time are schematically shown in *Fig. 5-6*.

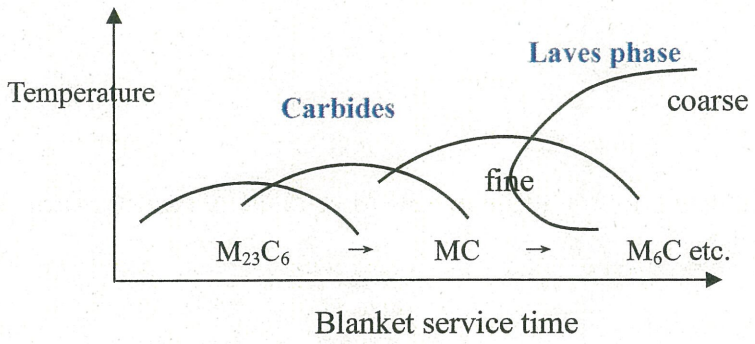

Fig. 5-6 Schematic illustration of the precipitates processes during blanket service time

5.3.2 Precipitates in the present ageing conditions

In the present study, the ageing experiments covered a relatively short time and the maximum time was up to 2000 h. The dominate precipitates were $M_{23}C_6$ ($Cr_{23}C_6$) and MC (TaC), as identified by EDS analysis. The precipitates of Laves and M_6C were not detected.

These results are consistent with those calculated data for F82H by Tanigawa (*Fig. 5-7*) [88], which showed that Laves phase began to appear over 873 K at TBM life time, and M_6C appeared at 773 and 823 over 10000 h. Our present ageing conditions are just before the formation of those phases, as shown as the solid yellow cycles in *Fig.5-7*.

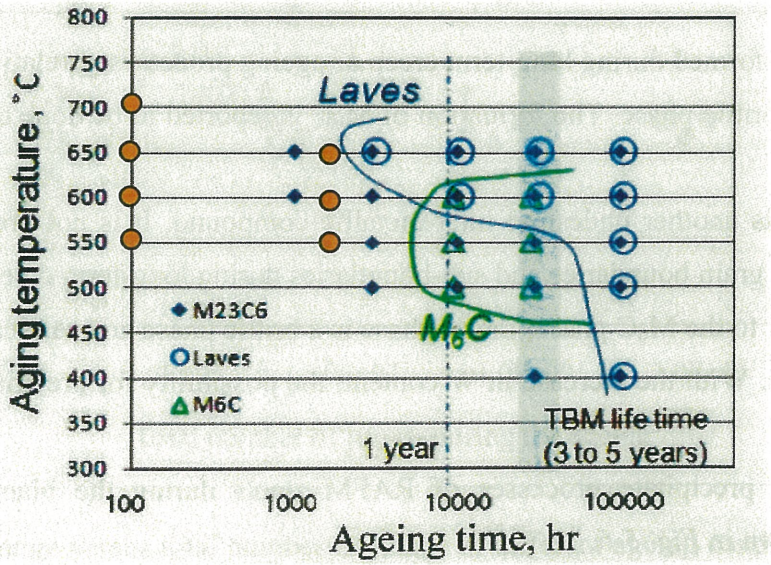

Fig. 5-7 Temperature-Time-Precipitates curves for F82H steels [88]
(●: the present ageing conditions for JLF-1 and CLAM in this study)

5.3.3 Precipitates kinetics during the ageing at 823 K

The amount of precipitates will change dependent on the ageing temperature and time. At the typical blanket maximum service temperature, 823 K, the dependence of precipitates with ageing time is plotted in *Fig. 5-8*, according to the obtained data in the Chapter 4.

The microstructure examination showed that, the total density exhibited an increase tendency with the ageing times from 0, 100 to 2000 h at 823 K. The increase of TaC can be considered as the reason for the most increase of total density of precipitates, as proved in Chapter 4.

Ageing for longer time, the density of precipitates is suggested to be saturated and then decreased, because of the possible coarsening and combining of precipitates. However, longer-term ageing experiment is needed to clarify the whole tendency of precipitates change.

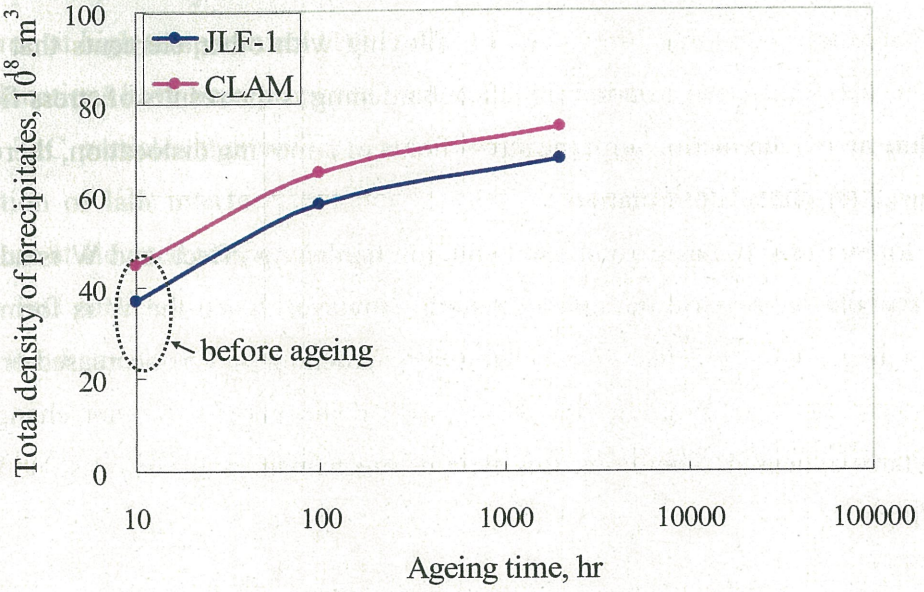

Fig.5-8 The dependence of total number density of precipitates on the ageing time at the typical blanket maximum service temperature (823 K) for JLF-1 and CLAM steels

5.4 Relation between the mechanical property change and microstructural evolution

The changes in mechanical property and the corresponding microstructural evolution by thermal ageing are summarized in *Table 5-2*. The detailed mechanisms for the change will be discussed in the following sections.

Table 5-2 The changes of mechanical properties and microstructure by thermal ageing

	823K/2000h	873K/2000h	923K/2000h	973K/100h
hardness	hardening ↑	softening ↓	softening ↓	softening ↓
tensile stress	small change	decreased ↓	decreased ↓	decreased ↓
creep stress	improved ↑	improved ↑	improved ↑	degraded ↓
precipitates density	increased ↑	increased ↑	increased ↑	decreased ↓

5.4.1 Possible hardening mechanism after ageing at 823 K up to 2000 h

Generally, there are several kinds of hardening mechanisms for metallic materials:

(1) Solid-solution hardening:

The solid-solution hardening is induced by alloying with other elements that go into either substitutional or interstitial solid solution [88]. The hardening is the results of stress fields generated around the solute atoms interacting with the stress fields of a moving dislocation, thereby increasing the stress required for plastic deformation.

It is well known that W has a good solid solution hardening effect, and W is added in RAFM steels for the purpose to increase the creep strength. However, when the W is formed into a new phase, such as Laves phase, the effect of solid-solution hardening will be decreased or be lost.

In the present ageing conditions, the W content in the matrix will not change because no W-rich precipitates appeared. Therefore, this type of mechanism will not cause additional effects during the ageing.

(2) Hardening by grain size reduction

The size of the grains, or average grain diameter, can influence the mechanical properties of a metal material [88]. The grain boundary can act as a barrier to dislocation motion during plastic deformation. The finely grained material has a greater total grain boundary area to impede dislocation motion. For many materials, the yield strength, hardness and toughness can be improved by reduction in grain size at the same time.

Grain size may be regulated by the cooling rate of solidification from the liquid phase, plastic deformation followed by an appropriate heat treatment, and also by addition of small amount of special elements.

In order to decrease the grain size and form the strong fine precipitates, Ta is added into the

RAFM steels. The higher content of Ta for CLAM may be one of the reasons for finer grain size and thus higher strength than that of JLF-1. This will be discussed on Section 5.5.

During the present thermal ageing, the growth of grain size was not remarkable. Therefore, the effect of grain size on the property also can be ignored.

(3) Precipitate hardening

The strength and hardness of some alloys may be enhanced by the formation of extremely small and uniformly dispersed particles of a second phase within the original phase matrix. Therefore, the fine dispersion of nano-scale particles is one of effective hardening mechanisms for the RAFM steels.

It was reported that the precipitate hardening of RAFM steels was mostly derive from the MC type precipitates, usually TaC, which can form much finer dispersion than $M_{23}C_6$ and Laves phase in bcc iron at high temperatures [106-107].

Two explanations have been proposed on the TaC hardening:

(1) The TaC particles themselves act as obstacles in the steels, which would prevent the migration of lath interface and pin down the motion of dislocations during long-term exposure at elevated temperature, leading to the increase in strength and hardness.

(2) The TaC particles can slow down recovery of the dislocation and lath substructure, and retain the dislocation hardening for longer duration.

After ageing at 823 K for 2000 h, the hardness and creep strength increased. From the microstructure observation, the total density of precipitates also increased. Particularly, the TaC precipitates newly formed during the ageing. Thus, the change in precipitates, especially in TaC, can be considered to be the main reason for the increase in hardness and creep strength by ageing at 823 K for 2000 h. The possible hardening mechanism is schematically demonstrated in *Fig.5-9*.

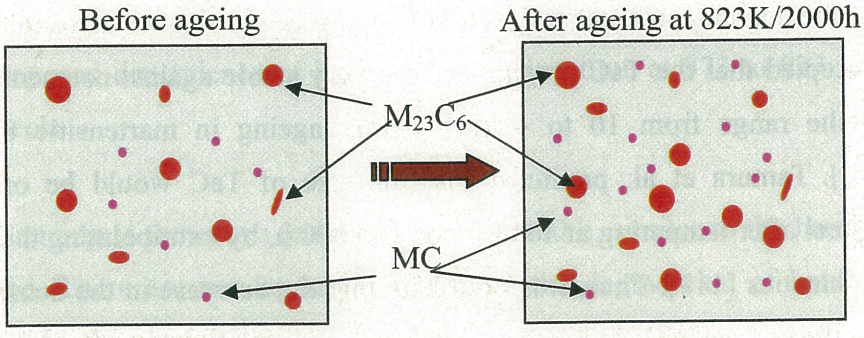

Fig. 5-9 Schematic illustration of the possible hardening mechanism by ageing at 823 K/2000 h

5.4.2 Possible softening mechanism by ageing at 973 K

The softening mechanisms for typical RAFM steels can be summarized: (a) dissolution of fine carbonitrides [108], (b) preferential recovery of microstructure in the vicinity of prior austenite grain boundaries [109], (c) recovery of excess dislocations [110], and so on.

The present results by TEM observation showed that the number density of small precipitates, TaC, decreased after ageing at 973 K for 100 h. However, the calculated results by disperse obstacle model showed that, the change in precipitates alone cannot explain for the change in hardness. Some other factors will also operate for the softening.

Furthermore, the recovery of martensitic laths and dislocations took place, which was also proved by TEM observation. The recovery also can contribute to the softening.

Therefore, the schematic illustration of the possible softening mechanism is shown in *Fig. 5-10*.

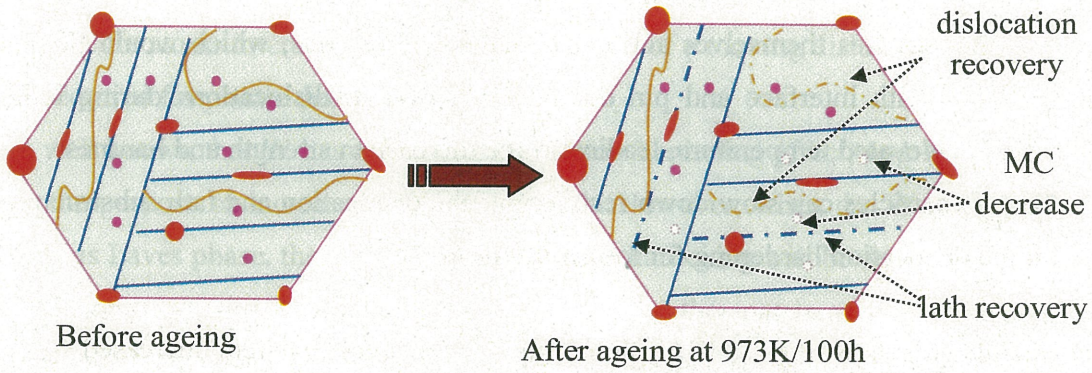

Fig. 5-10 Schematic illustration of the possible softening mechanism by thermal ageing at 973 K for 100 h, the dotted markers show the loss and recovery.

The number density of fine TaC decreased by ageing at 973 K for 100 h. There are two possible ways for the decrease in number density of small TaC: growth or dissolution.

It is well accepted that the TaC precipitates are very stable against coarsening, and with a typical sizes in the range from 10 to 40 nm before ageing in martensitic 8-12%Cr steels [106-107,111-112]. Tamura et al. predicted that the size of TaC would be only 39 nm for Fe-8%Cr-2%W steel after tempering at 1013 K for 100 000 h, by extrapolating the available data using coarsening kinetics [111]. Thus, it is not likely that the decrease in the density of fine TaC particles is due to the coarsening.

On the other hand, the TaC precipitates formed mainly on dislocations and other defects [111]. When dislocations annihilate or move from the precipitates, the precipitates may become unstable and be dissolved. The similar phenomena have been reported in martensitic steel precipitating NbC [113]. The present experiments showed that the overageing at 973 K for 100 h caused a recovery of microstructure, enhancing the dissolution of TaC. However the contribution of the precipitates recovery to the softening was small relative to the other microstructural recovery.

5.4.3 The mechanisms for the property changes by ageing temperature at 873 and 923 K

The hardness decreased after ageing at 873 and 923 K, but the decrease was almost independent on the ageing time, as discussed in Figs.5-4 and 5-5 by thermal activation energy analysis. This implies that the softening in the present steels took place only in the initial ageing time, as schematically shown in *Fig. 5-11*. In this case, further softening needs formation of new phases, such as Laves and M_6C phases.

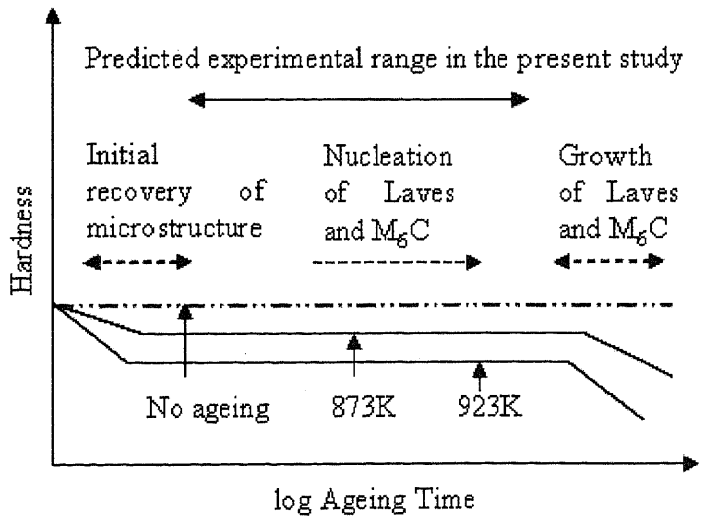

Fig. 5-11 The proposed dependence of hardness on ageing time at 873 to 923 K for JLF-1 and CLAM steels.

In addition, ageing at these two temperatures for 2000 h, similar to the hardness, the tensile strength decreased. There are two opposite effects for the degradation of hardness and tensile strength. On one side, the precipitates increased, which would lead to hardening. On the other side, the recovery of laths and dislocations would result in softening. Since precipitates change took

small positive effect, while the recovery took the larger negative effects, the hardness and tensile strength was decreased as a result.

Different from the hardness and tensile, the creep property improved and density of precipitates increased. Thus, it seems that, the increase in TaC precipitates was the dominant factor to enhance the creep properties.

5.5 Comparison of JLF-1 and CLAM steels

5.5.1 Higher hardness and strength of CLAM than those of JLF-1

The results of mechanical property tests showed that the hardness, tensile and creep strength of CLAM were higher than those of JLF-1, which can be explained by corresponding microstructure resulted from the heat treatment conditions and chemical compositions.

The main microstructural difference before ageing in the both steels appeared to be the prior austenite grain size and the lath width, which could account for the difference in hardness and strength.

It is well known that smaller grain size can lead to the higher yield strength, based on the Hall-Petch's equation [114]:

$$\Delta\sigma_y = k_b \times \Delta D^{-1/2} \qquad (5\text{-}4)$$

where

σ_y = the yield strength,

k_b = the constant relating interaction between grain boundary and dislocation,

D = the grain diameter.

Here the effect of grain size could be estimated roughly according to the above equation.

Because RAFM steels have anisotropic and very fine lath structure, it is difficult to determine the effective D. In Ref. [115], the packet diameter was thought as more acceptable for D than the prior austenite grain diameter. The packet boundaries consist of both prior austenite grain boundaries and lath boundaries. While in Ref. [116], the average lath diameter was suggested to be the effective D in the case of the lath structure considering the length of the slip plane in the lath. Because there were not 100% lath-martensitite for CLAM and JLF-1 steels, and

the packet diameter and length were hard to be determined, the prior austenite grain diameter was used to estimate the difference in YS between CLAM and JLF-1 steels.

The grain size for CLAM steel was about 6 μm before ageing, which was almost half of that (10μm) for JLF-1 [67]. Factor k_b was determined to be 0.62 $MNm^{-1.5}$ according to Ref. [117]. So the difference in YS between CLAM and JLF-1, $\Delta\sigma_y$, had been calculated to be about 67 MPa, in good agreement with the difference of 65 MPa, obtained by the experiments.

One of the possible reasons for finer prior austenite grain size and lath width of CLAM is the effects of different heat treatments. Some earlier studies have shown that mechanical properties can be varied by variations of the normalization (quenching) temperature and the tempering temperature [118]. In this case, the normalization was 1253 K for 30 minutes for CLAM, while 1323 K for 60 minutes for JLF-1. Lower normalization temperature and shorter time for CLAM leaded to finer prior austenite grain. In addition, the tempering temperatures were 1033 K for CLAM and 1053 K for JLF-1. The lower tempering temperature would cause the smaller lath width. Therefore, these two factors would results in the higher hardness, tensile and creep strength for CLAM.

The other possible reason for finer prior austenite grain size and smaller lath width is the effect of the element Ta. It has been reported that the Ta has a beneficial effect on DBTT and strength [119]. In the 9Cr-2W steel, the addition of 0.05%Ta presented finer grain sizes for all the normalization temperatures from 1223 K to 1423 K, and caused the increase in the strength at elevated temperatures and the decrease in the toughness at low temperatures [119]. The positive effect of Ta was also observed in other 5Cr and 9Cr steels [120]. Ta, like Nb, is a strong carbide former, and can retard the growth of austenite in heating process and inhibit austenite grain growth. CLAM steel contained 0.15%Ta as alloying elements, which was higher than that of JLF-1 (0.083%Ta). The higher content of Ta is considered as the other possible reason for finer microstructure.

In addition, during the present creep stress range where the dislocation rather than the diffusion mechanism operated, the higher tensile strength of CLAM steel is thought to be the reason for the lower minimum creep rate and longer rupture time than those of JLF-1.

5.5.2 Higher susceptibility to thermal ageing of CLAM than that of JLF-1

Although the CLAM has higher hardness, tensile and creep strength, the differences in these properties between aged and unaged conditions were larger than those of JLF-1.

The present study revealed that, because of lower heat treatment temperature, CLAM steel would be more susceptible to thermal ageing than JLF-1. Thus, it was indicated that the present heat treatment condition for CLAM may not the best one. The further optimization of heat treatment conditions by increase in temperature should be improved for CLAM in the future.

5.6 The status of Ta in RAFM steels

As mentioned in the previous chapter, Ta is a new element used in RAFM steels, instead of Nb in the traditional steels which can cause the long radioactivity. Although some research has been done about the status of Ta in steels, the history is very short.

Totally, the effects of Ta on property for RAFM steels have two opposite aspects:

(1) The positive effects on property

Ta is a solid-solution hardening element, which can limit the growth of austenitic gain, leading to the increase in yield strength and toughness at the same time.

The effect of Ta on grain size and DBTT has been proved by Alamo [121] and Tanigawa et al. [122], as shown in *Fig.5-12* and *5-13*. The alloys with less than 0.1%Ta have a finer grain size.

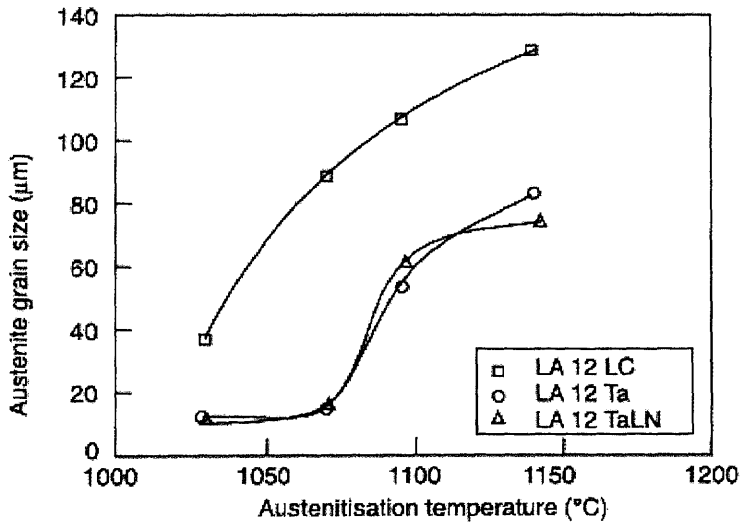

Fig.5-12 The effect of Ta on austenite grain size for low activation alloys (The content of Ta was 0.01%, 0.10% and 0.10% for LA12LC, LATa, and LA12TaLN, respectively) [121].

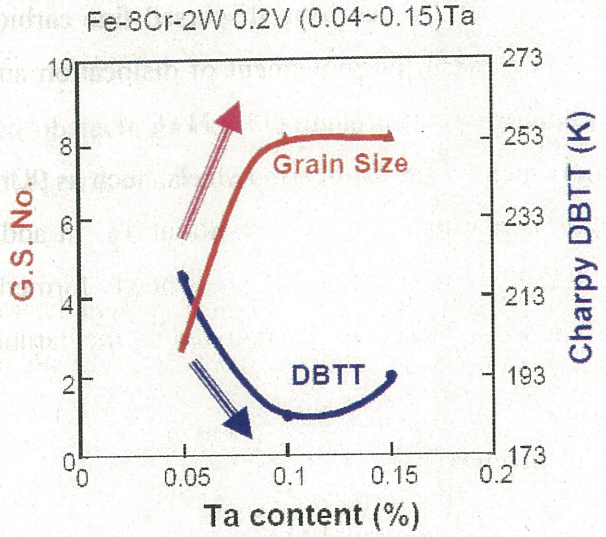

Fig.5-13 Effects of Ta content on grain size and DBTT (G.S.No.: grain size number) [122]

The opposite effect of Ta was also found in the previous and present study for CLAM. CLAM steel has higher level of Ta, and thus leading to the lower DBTT *(Fig. 5-14)* and higher yield strength than those of JLF-1, as discussed in Chapter 5.5.

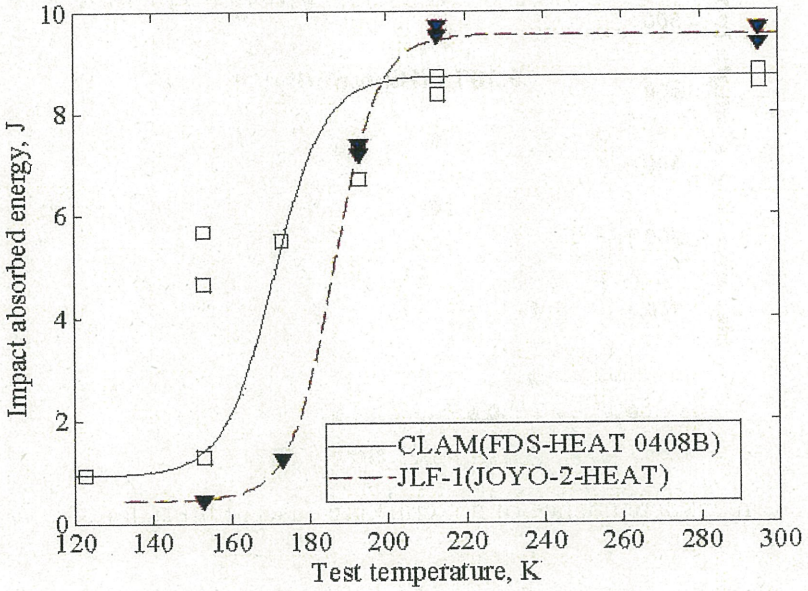

Fig. 5-14 Impact absorbed energy – test temperature curves for JLF-1 and CLAM steels, showing the lower DBTT of CLAM than JLF-1 (The content of Ta is 0.15% and 0.083% for JLF-1 and CLAM, respectively). [67]

Another important aspect is that, Ta can form dispersed fine carbides of the MX type with nitrogen and carbon, which can prevent the movement of dislocation and transfer of martensitic lath interface, thus leading to higher creep strength [110-111].

This effect was also confirmed by the Ta-bearing steels, such as 9Cr-2WVTa, JLF-1, CLAM showed higher creep strength as compared to steels without Ta. In addition, this study showed that, after thermal ageing at 823 K for 2000 h, the TaC was newly formed. The formation of small TaC also caused positive effects on the hardening, as proved by the hardness measurement.

(2) The negative effects on property

Ta is also the element which was found to decrease the mechanical property of weldment. As reported by Tanigawa et al. [122], the cracking resistance at high temperature decreased with the increase of Ta content above 0.1%, as shown in *Fig. 5-15*.

In addition, the present study found that, the small TaC precipitates are unstable, which can newly form or disappear by dissolution after ageing at 973 K, as shown in Chapter 4. This is a new finding, which can provide the valuable information to further evaluate the effect of Ta.

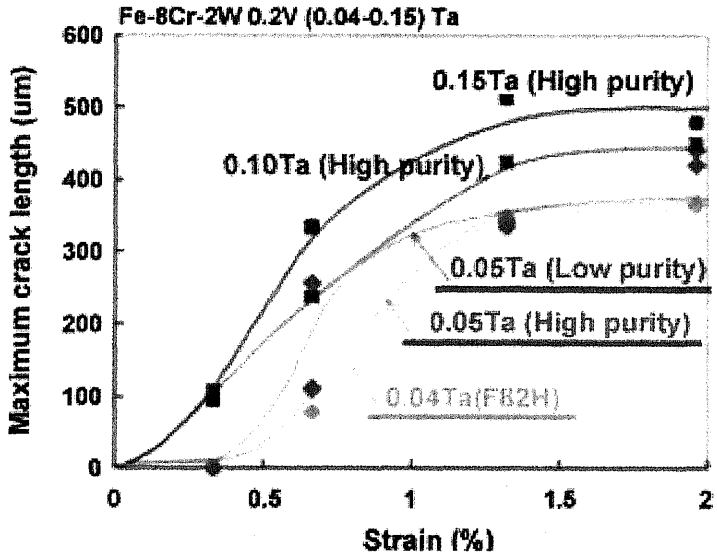

Fig. 5-15 Ta content dependence of hot cracking susceptibility for RAFM steels [122].

Generally, Ta has not been used for commercial alloys up to now, and only used in RAFM steels for fusion application. As a result, there is lack of information, compared to the other steel alloying elements. The extensive research on the fate of TaC and the further optimization of chemical composition considering the behavior of TaC is necessary for RAFM steels.

5.7 Summary

1. A traditional dispersed obstacle model was used to correlate the hardness and microstructure changes. In the present ageing conditions, the dominate obstacle was assumed to be precipitates only.
2. The calculated hardness change by this model agreed well with the measured data for ageing at 823 K/2000 h. Thus, the formation of TaC was considered to be the main reason for the observed hardening due to ageing.
3. However, there was a large difference between the calculated and measure dada for ageing at 973 K/100 h, indicating that the loss of TaC alone cannot account for the softening according to the dispersed obstacle model. The recovery of dislocations and lath structure can contribute the major effects to the softening for ageing at 973 K for 100 h.
4. From the activation energy analysis, the total number of jumps was not an appropriate correlation parameter in any case of the activation energy. This means that the hardness change by ageing is not the thermally activated process with particular activation energy.
5. The present ageing conditions seems to be located after the initial microstructural recovery, and before the formation of Laves and M_6C phases, which are the undesired brittle phases.
6. The lower heat treatment temperature and higher content of Ta for CLAM steel was considered as the reasons for higher hardness, tensile and creep strength than those of JLF-1. However, because of lower heat treatment temperature, CLAM steel was more susceptible to thermal ageing than JLF-1.
7. The present results suggest that, the heat treatment condition for CLAM should be improved.
8. Ta is a new element used in RAFM steels instead of high radioactivity element Nb. Ta can has positive effects on some property, and also has sometimes negative effects on some property. The understanding of the status of Ta is very limited.
9. The present study found that TaC precipitates were unstable, which can form newly or disappear by dissolution during the thermal ageing. The extensive research on the fate of TaC and the further optimization of chemical composition considering the behavior of TaC is necessary for RAFM steels.

CHAPTER 6

Prediction of Creep Rupture Performance in The Typical Blanket Condition

6.1 The methods for prediction of long-term creep behavior

Since structural materials are subjected to long-term loading at high temperature, it is necessary to evaluate the creep behavior over the long-term service. However, measurements of the rupture properties at actual low stress condition are very costly and time-consuming. Thus the suitable extrapolation method to estimate the creep property is highly desired.

For this purpose, generally there are three key methods: stress-rupture, minimum creep rate vs. rupture time, and temperature compensated time.

(1) Stress-rupture

In this method, a large number of tests are needed to be carried out at various stresses and temperatures to develop plots of applied stress versus rupture time, as shown in *Fig. 6-1*.

It is relatively easy to use these plots to provide estimates of rupture life or rupture stress within the range of stresses and lives covered by the test data. However, when the failure mechanism changes as a function of time or stress, as shown by the "knee" in the figure, extrapolation of the data can be problematic [88].

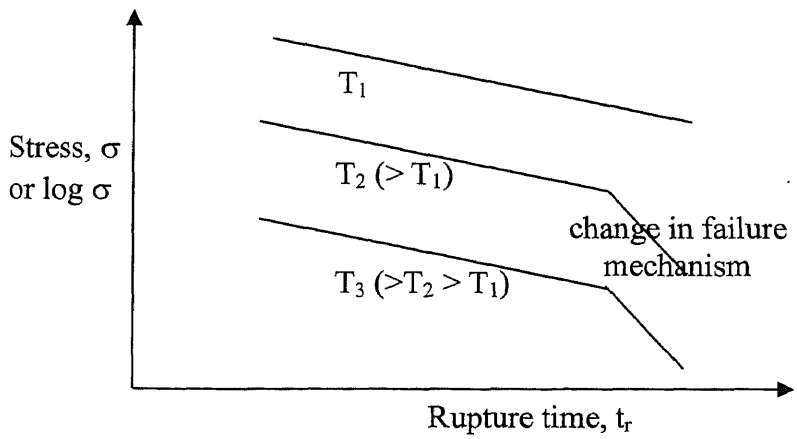

Fig. 6-1 Stress - rupture time plot for various temperatures [88]

(2) Minimum creep rate - rupture time

Another method to extrapolate the results of accelerated creep tests is Monkman-Grant (M-G) relation, for a given materials in a certain range of stress and stain.

The Monkman-Grant relation has the following equation [123]:

$$r_{\min} \times t_r = C \qquad (6\text{-}1)$$

where r_{min} is the minimum creep rate, t_r is the rupture time, and C is the constant.

On a Monkman-Grant plot, log-log plot of r_{min} versus t_r, as shown in *Fig.6-2*, prediction of the rupture time is possible by measuring the minimum creep rate at a given stress and temperature. This equation often holds true, but in some cases it will lead to an overestimation of the creep rupture life at low stresses.

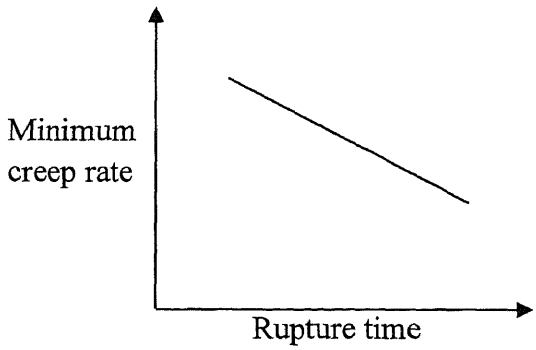

Fig. 6-2 Minimum creep rate - rupture time plot

(3) Temperature-compensated time

Larson-Miller parameter (LMP) is one of the very simple methods [124]. In this method, the test data at higher temperature with short rupture time are used. Extrapolation of creep rupture stress based on the results of short-term creep testes is possible by this parameter, as shown in *Fig. 6-3*.

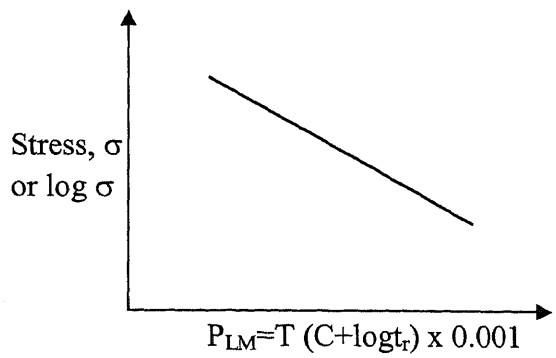

Fig. 6-3 Stress – Larson-Miller parameter plot

The stress dependence of the creep rate and the rupture time as a basis for extrapolation of the rupture stress have been frequently investigated for precipitation strengthened ferritic steels used in fission reactors [125]. However, limited data are available for RAFM steels [126]. No effort has been made to include the thermal aging effect on the prediction of the long-term creep performance of RAFM steels.

In this work, the method for predicting the stress limit in typical blanket condition, 823 K for 100000 h, will be proposed and the results will be reported and discussed.

6.2 Prediction of creep performance in typical blanket condition by Monkman-Grant equation

It was reported that using the Monkman-Grant (M-G) equation [123] together with the Norton law [91] can predict the creep properties of 9%Cr steels.

Taking the logarithm of both sides for the equation 6-1, then:

$$\log r_{\min} = -1/n \times \log t_r + D \qquad (6\text{-}2)$$

where n and D are the constants.

In this study, this method will be attempted to predict the long-term creep performance in typical blanket condition, firstly.

Figs. *6-4* and *6-5* present the minimum creep rate (r_{min}) as a function of rupture time (t_r) on log-log scale for JLF-1 and CLAM steels, respectively.

By extending the data to the typical blanket time, 100 000h, the minimum creep rate can be obtained. Then, with the obtained minimum creep rate, and from the plot of minimum creep rate vs. applied stress, the Norton law, the corresponding rupture stress can be found.

However, since the present creep experiment covered only a narrow range, the error by the extrapolation looks very large.

In spite of that, the figures show that the constant n was almost equal to 1, which is useful for our next prediction.

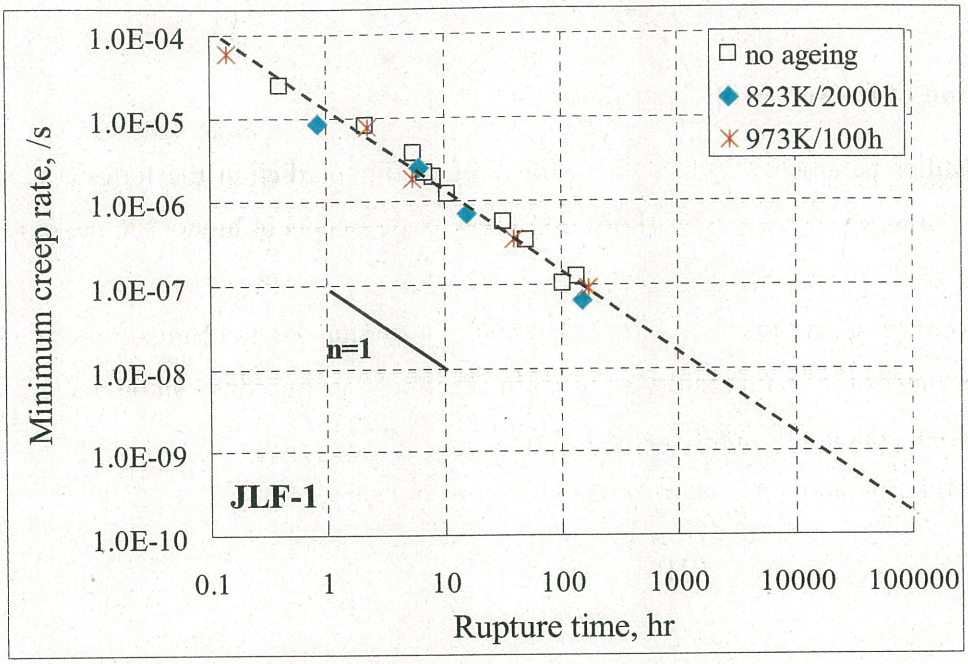

Fig. 6-4 Minimum creep rate as a function of rupture time (M-G equation) for JLF-1 steel.

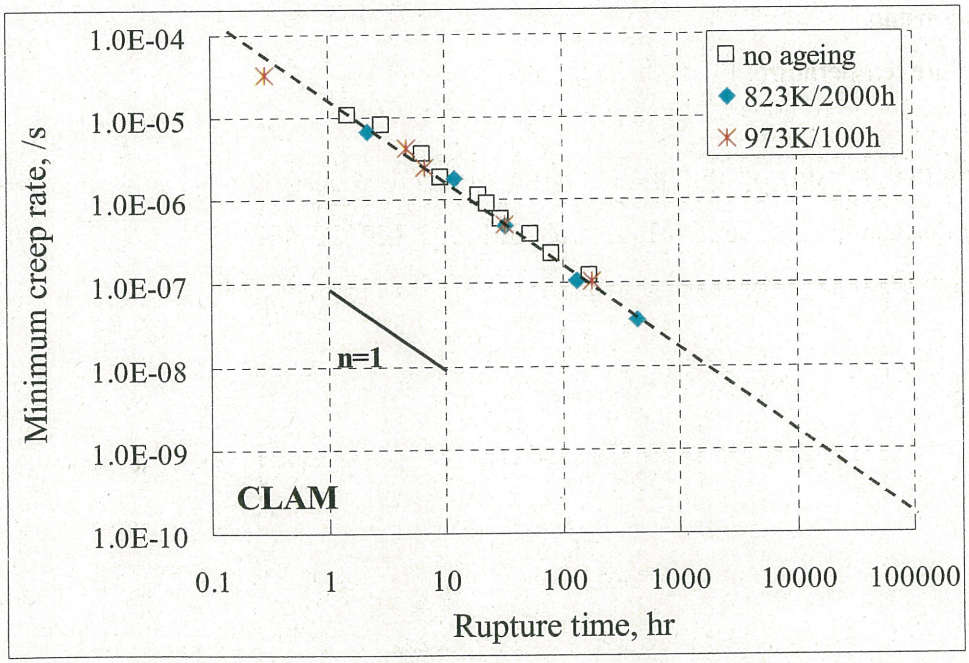

Fig. 6-5 Minimum creep rate as a function of rupture time (M-G equation) for CLAM steel.

6.3 Prediction of creep performance in typical blanket condition by Larson-Miller Parameter

6.3.1 Definition of Larson-Miller parameter

Larson-Miller parameter is one of popular method for prediction the long-term creep rupture performance, based on the results of short-term creep experiments at higher temperature with higher stresses.

In this form of accelerated tests, it is assumed that the failure mechanism does not change and hence is not a function of temperature or time. In addition, assumptions can be made that activation energy (Q) is independent of applied stress.

Larson-Miller parameter is based on the model of the rate processes [124]:

$$r_{min} = A \times \exp(-Q / RT) \qquad (6\text{-}3)$$

where

r_{min} = minimum creep rate

A = constant

exp = natural logarithm base

Q = activation energy for process

R = gas constant

T = absolute temperature, K

Assuming that the time of primary and tertiary creep is much shorter than that of the secondary creep, and the tertiary creep begins when total strain reached a critical value (ε_r), the creep curve is simplified as schematically presented in *Fig. 6-6*.

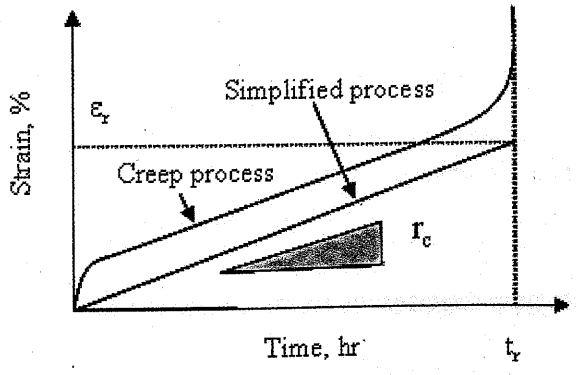

Fig. 6-6 Schematic illustration the creep curve and simplified process

In this case, there is a relation as expressed in eq. 6-4:

$$r_{\min} = \varepsilon_r / t_r \qquad (6\text{-}4)$$

where t_r is the rupture time, hour.

Comparing eq. 6-2 with n of 1, D in eq. 6-2 is $\log \varepsilon_r$. Thus, the eq. 6-3 can be written as:

$$1/t_r = A/\varepsilon_r \times \exp(-Q/RT) \qquad (6\text{-}5)$$

Taking the logarithm of both sides for eq. 6-5, then:

$$T(C + \log t_r) = Q/2.3R \qquad (6\text{-}6)$$

Finally, the Larson-Miller parameter (LMP) can be described as:

$$LMP = T(C + \log t_r) \times 0.001 \qquad (6\text{-}7)$$

where C is the constant of materials.

This relation shows that the two parameters, temperature (T) and rupture time (t_r), can be combined into one equation. In addition, the data by short-term experiment at higher temperature can be used for predicting those by long-term experiment at lower temperature.

LMP assumes that temperature and time can be interchanged, provided no important microstructural changes occurred during the test. When the creep mechanism changes, the use of this parameter for predicting long time performance is not accurate. In the present study, the microstructure was assumed not to change.

6.3.2 Determination of the C value

The C in Larson-Miller equation is a material constant. Firstly, C value will be determined.

In this study, a wide range of C values from 10 to 40 were used for the same creep data before ageing to obtain the suitable C value. The fitting lines for the both steels are shown in *Fig.6-7*. From the figure, it was found that the C of 30 was suitable for the both steels, because most data are almost on the smooth straight lines.

Originally, for conventional tempered steels, C is assumed to be 20 by Larson and Miller [124]. Usually, the C of 30 is used for EUROFER 97 steel, [86] and 28 for F82H steel [86].

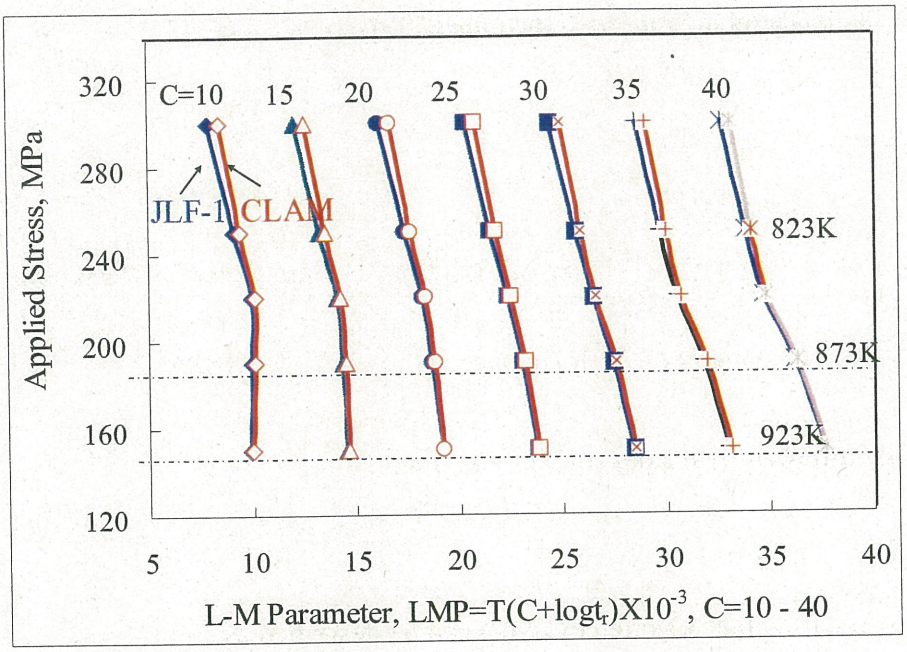

Fig. 6-7 Fitting of the Larson-Millar parameter with applied stress for various values of C from 10 to 40 for JLF-1 and CLAM steels before ageing

6.3.3 Prediction of creep performance in typical blanket condition without ageing effects

The blanket will be operated for several decades. In typical design for the blanket using the RAFM steels, the expected blanket operation limit would be 823 K and 100 000 h. Thus, the prediction of the materials performance to the operation limit is very important for RAFM steels to apply in fusion reactors.

The experimental data at different temperatures with applied stress are plotted in *Fig.6-8*. Prediction based on the Larson-Miller parameter with the determined C value (30) is also shown in the figure. According to the new creep theory [127], the stress axis is plotted in a linear scale, not in a logarithm scale by the traditional method.

In the typical blanket condition, 823 K for 100 000 h, the Larson-Miller parameter equals to 28.8, according to the *equation 6-8*.

$$LMP = 823(30 + \log 100000) \times 0.001 \qquad (6\text{-}8)$$

By prediction (Fig.6-8), the rupture stress was estimated to be about 140 MPa for the both steels. Based on ASTM VIII guideline, the acceptable stress limit of $2/3 \times 140 = 93MPa$ is derived for the both steels considering the safety factor for design.

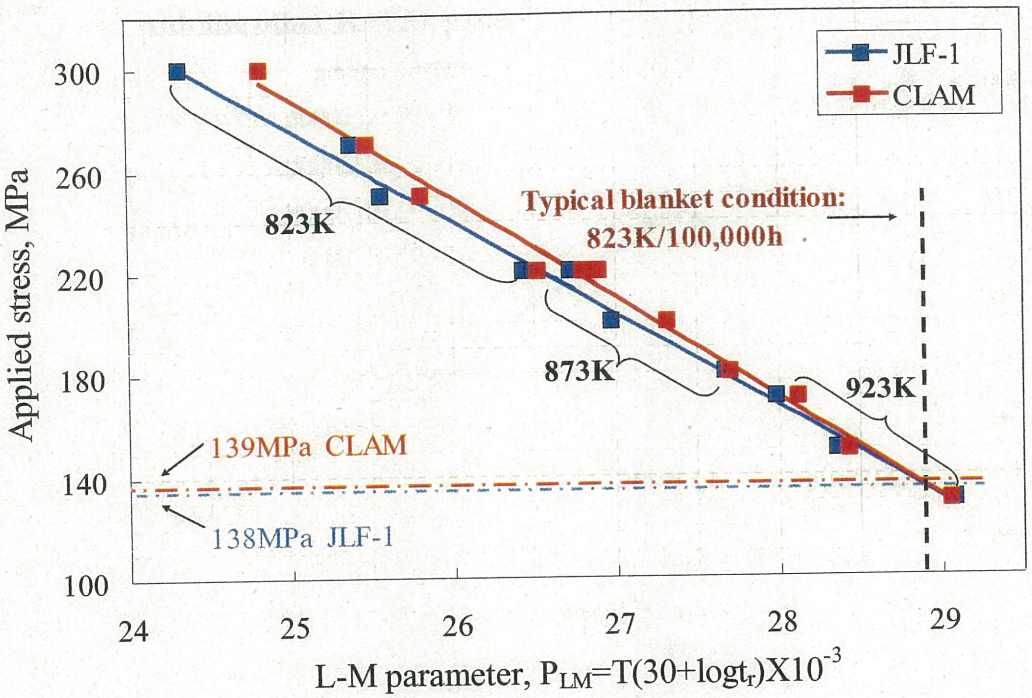

Fig. 6-8 The dependence of Larson-Miller parameter on applied stress.

6.3.4 Prediction of creep performance in typical blanket condition including ageing effects

The present study showed that the pre-ageing can influence the creep properties. Because the creep tests already involve some ageing effects, it is not easy to estimate the stress effects and the ageing effects separately from the creep tests.

The correlation with LMP includes only partial effects of property change by ageing. The LMP correlation with pre-aged specimens can be useful for predicting the overall effects of the ageing.

The applied stress dependent on Larson-Miller parameter is shown in *Figs. 6-9* and *6-10*, for JLF-1 and CLAM, respectively.

The diagrams show the increase of Larson-Miller parameter by ageing at 823 and 873 K and the decrease by ageing at 973 K for the both steels.

In the typical blanket condition, 823K/100 000h, the estimated rupture stress can be changed by about ±10 MPa by the pre-ageing. This sort of variation needs to be considered as the possible thermal ageing effects during the thermal creep processes.

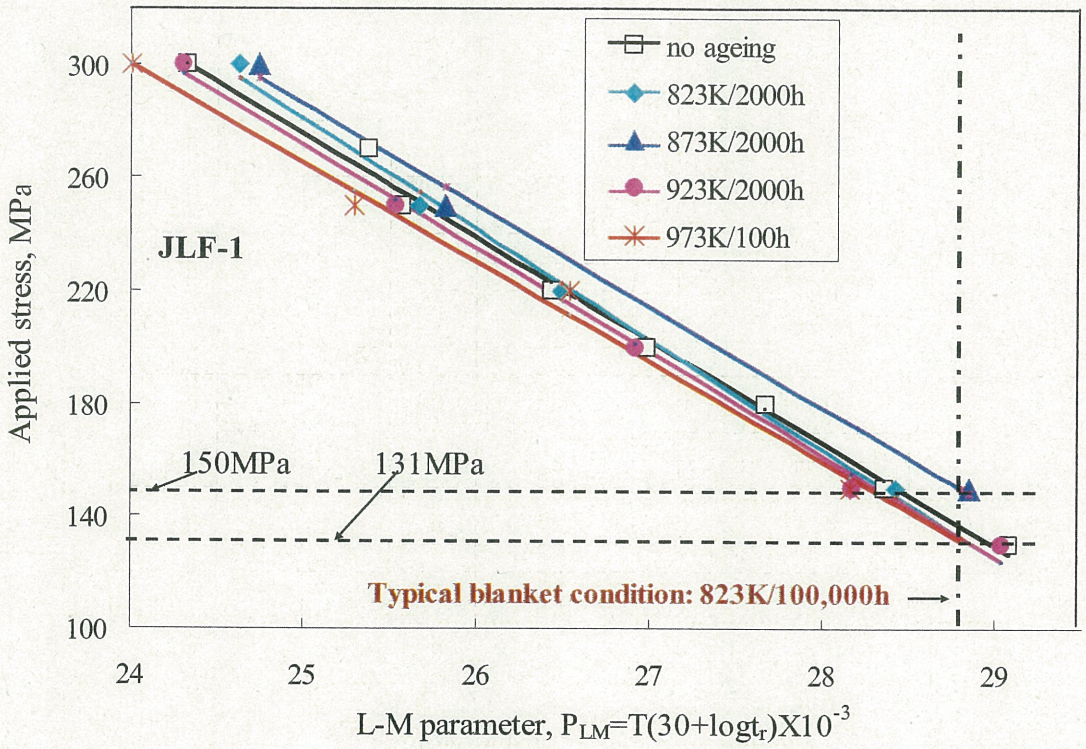

Fig. 6-9 The applied stress as a function of Larson-Millar Parameter for JLF-1.

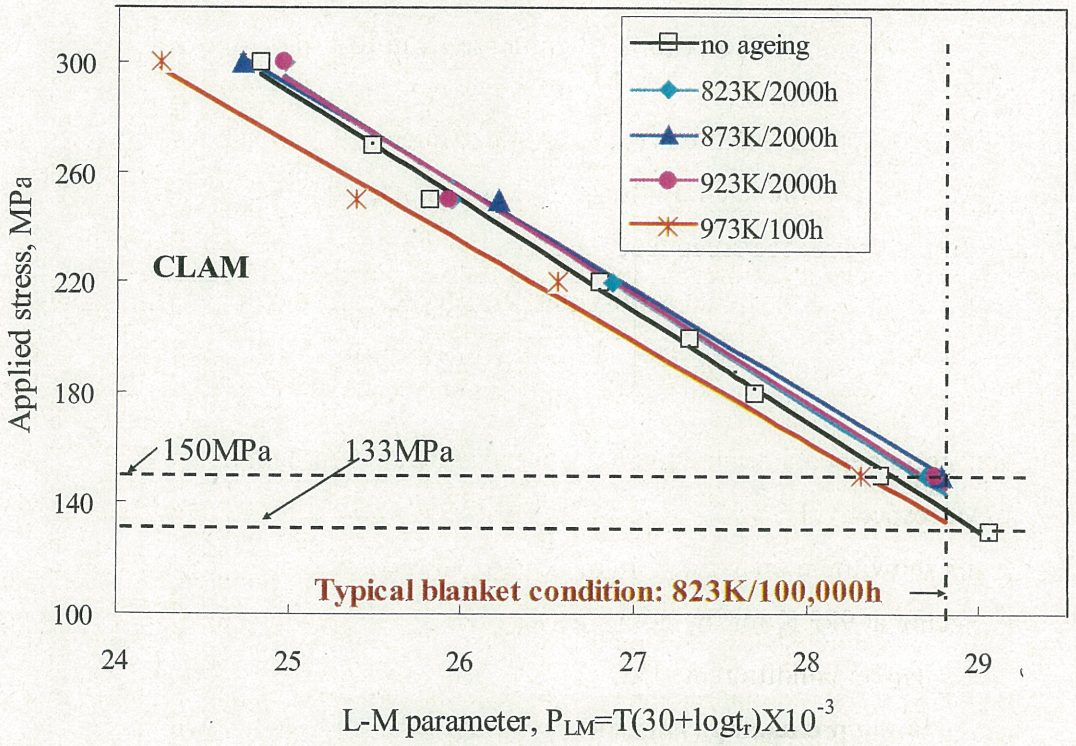

Fig. 6-10 Applied stress as a function of Larson-Millar Parameter for CLAM steel.

6.3.5 Comparison with the other RAFM steels

A lot of creep tests were carried out for EUROFER 97 at 723-923K for period up to 10000 h and some were expected to cover rupture times between 20000 - 40000 h. The results of the creep experiment are shown in *Fig. 6-11*, with the comparison of OPTIFER, F82H-mod, and ODS-EUROFER [85].

The figure shows that our predicted rupture stress for JLF-1 and CLAM are comparable to those of other RAFMs, such as EUROFER 97, F82H, but lower than that of ODS steels.

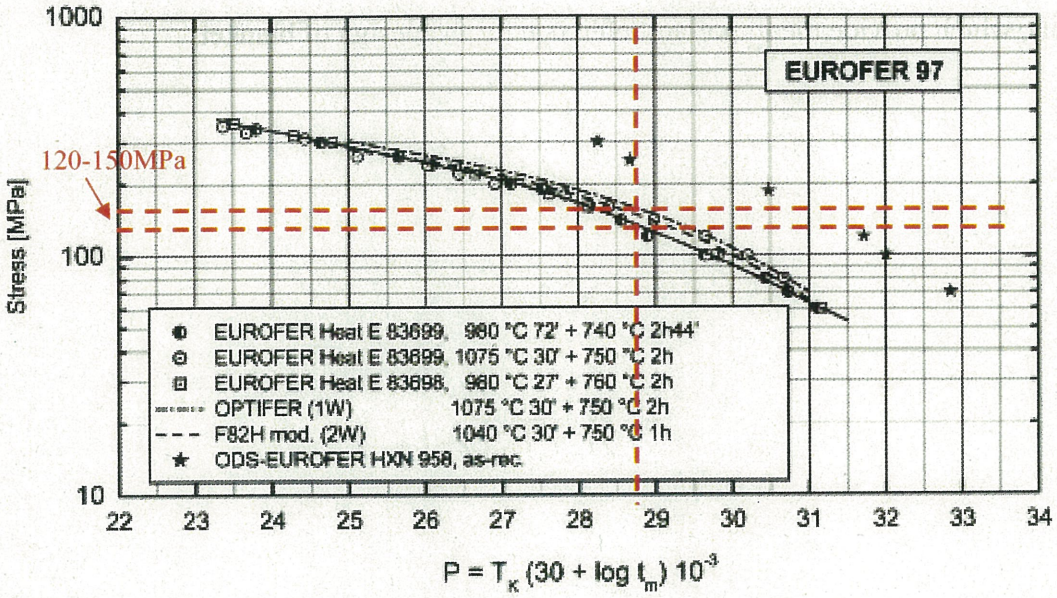

Fig. 6-11 Larson-Miller Plot for EUROFER 97 bar and plate material with different heat treatments, in comparison with OPTIFER developmental alloy, F82H-mod and ODS-EUROFER [85] (The P is equal to 28.8 in typical blanket condition, 823K/100000h).

6.4 Summary

1. The different methods for predicting the creep performance in typical blanket condition, 823 K for 100 000 h, were attempted in this study.
2. The prediction results by using the Monkman-Grant equation showed that the error looked large. However, the results revealed that n value in this equation was almost equal to 1.
3. Larson-Miller parameter was useful and successful to predicting the long-term creep

performance based on the short-term experiments at higher temperature in this study.

4. The estimated rupture stress by Larson-Miller parameter was about 140 MPa for the both steels.

5. Since the Larson-Miller parameter only covered partial ageing effect, the pre-ageing experiments before creep in present study were applied for prediction of the rupture stress including the overall ageing effects.

6. The present ageing treatment will influence the rupture stress by about ±10 MPa for the both steels, which provide the important reference for the design of blanket.

CHAPTER 7

Conclusions

RAFM steels are considered as the primary candidates of blanket structural materials for fusion reactor, because of the most matured technology base and good resistance to neutron irradiation. JLF-1 and CLAM steels are the reference alloys developed in Japan and China, respectively. The qualification of these RAFM steels for practical application requires an exhaustive understanding of their microstructure and mechanical properties. Of special relevance is ageing resistance behavior under long-term loading at high temperatures. Long-term thermal ageing may change the mechanical properties and recover the microstructure, leading to the decrease in the maximum operation temperature.

For this purpose, the ageing experiments for JLF-1 and CLAM steels were carried out at temperature from 823 to 973 K with a period up to 2000 h. The mechanical properties including hardness, tensile and creep have been tested, and the microstructural evolution was observed. The relation between mechanical property change and microstructural evolution by thermal ageing was investigated, and the mechanisms were discussed. In addition, prediction of the creep rupture performance in the typical blanket conditions was conducted including the effects of thermal ageing by M-G equation and L-M parameter.

The results of the present study are summarized as followed:

1. The hardness increased slightly after thermal ageing at 823 K for 100 to 2000 h for the both steels. However, ageing at higher than 823 K caused a decrease in hardness.

2. The tensile strength did not change much after ageing at 823 K for 2000 h for the both steels. However, ageing at higher than 823 K caused a decrease in tensile strength.

3. The creep property (minimum creep rate and rupture time) improved after ageing at 823 and 873 K for 2000 h. However, it degraded significantly after ageing at 973 K for 100 h.

4. The microstructure of the both steels exhibited the mixtured structure of lath- martensite and tempered-martensite with dense of dislocations and two types of precipitates, $M_{23}C_6$ and TaC.

5. The analysis of microstructural evolution showed that, the total density of precipitates increased at 823 to 923 K up to 2000 h, mostly because of the increase of small size precipitates (<80 nm). However, the total density of precipitates decreased after ageing at 973 K for 100 h, which was resulted from the decrease of small size precipitates.

6. The EDS analysis identified that, most of the small precipitates (<40 nm) were Ta-rich carbides (TaC), and larger precipitates were Cr-rich carbides ($M_{23}C_6$).

7. Analyzed by the dispersed obstacle model, the calculated hardness change almost agreed with

the measured data after ageing at 823 K for 2000 h, suggesting the formation of fine TaC was the main reason for hardening due to ageing.

8. However, there was a large difference between the calculated data by model and measured data after ageing at 973 K for 100 h, indicating the loss of TaC alone cannot account for the softening. The recovery of dislocations and lath structure can contribute the major effects to the softening.

9. The change in creep property by ageing had the similar tendency to the change in precipitates density, implying that the precipitate evolution dominated the change in creep property.

10. From the activation energy analysis, the total number of jumps was not an appropriate correlation parameter in any case of the activation energy. This means that the hardness change by ageing is not the thermally activated process with particular activation energy.

11. The present ageing conditions seems to be located after the initial microstructural recovery and before the softening by formation of Laves and M_6C phases.

12. The hardness, tensile strength, and creep stress of CLAM were higher than those of JLF-1. However, these properties of CLAM were also more susceptible to thermal ageing than those of JLF-1.

13. The lower heat treatment temperature and higher content of Ta for CLAM steel were considered as the reason for finer grain size and smaller lath width, and thus leading to the higher hardness, tensile and creep strength for CLAM than those of JLF-1. However, because of lower heat treatment temperature, CLAM steel was more susceptible to thermal ageing than JLF-1, suggesting the heat treatment condition for CLAM should be improved in the future.

14. By prediction with Larson-Miller parameter, the rupture stress at typical blanket condition, 823 K for 100 000 h, was estimated to be ~140 MPa for the both steels.

15. In this condition, the present thermal ageing can influence the predicted rupture stress by about ±10 MPa for the both steels. This sort of variation needs to be considered as the possible ageing effects during the creep processes.

One of the most important findings is that, TaC precipitates were unstable during the ageing, which can form newly or disappear. Ta has not been used for commercial alloys, and only used in

RAFM steels for fusion application. Ta can cause positive effects on some properties, and sometimes also produce the negative effects on some properties. Up to now, the understanding of status of Ta is very limited. The detailed research on the fate of TaC and the further optimization of chemical composition considering the behavior of TaC is necessary for RAFM steels.

Since the Larson-Miller parameter only involved partial ageing effects, the pre-ageing experiments in this study can provide the suggestion for developing suitable methods to predict the creep performance in blanket conditions including overall ageing effects. The present results can provided the valuable information for the stress design at high temperature for blanket using the RAFM steels.

The present ageing conditions were only covered the precipitation phases of $M_{23}C_6$ and MC. The research of longer-term ageing with the formation of Laves and M_6C phases should be considered in the future.

REFERENCES

[1] IEA "Key World Energy Statistic", (2007)

[2] D. L. Klass, *Energy Policy*, 31 (2003) 353-367.

[3] E. Claussen, V. A. Cochran, and D. P. Davis, *Climate Change: Science, Strategies, & Solutions,* University of Michigan, p. 373, 2001.

[4] J. Goldemberg, "The promise of clean energy", *Energy Policy,* 2005, in press.

[5] B. Little, "Long-Term Sustainabilitv of Nuclear Fission Energy", American Nuclear Society, *Annual Meeting,* 2006.

[6] K. Fiore, "Nuclear energy sustainability: Understanding ITER2", *Energy policy,* 34 (2006) 3334-3341.

[7] Y. Lechon, et al., "A global energy with fusion", *Fus. Eng. Des.*, 75-79 (2005) 1141-1144.

[8] J. Ongena, G. Van Oost, "Energy for Future Centuries - Prospects for Fusion Power as a Future Energy Source", *Fus. Sci. Tech.* 49 (2006) 3-15.

[9] ITER homepage, www.iter.org.

[10] S. Atzeni, J. Meyer-ter-Vehn, *The physics of inertial fusion,* Oxford University Press, ISBN 0198562640, 2004.

[11] C.M. Braams, P.E. Stott, *Nuclear Fusion: Half a Century of Magnetic Confinement Research.* Institute of Physics Publishing. ISBN 0-7503-0705-6. (2002).

[12] D. Maisonnier, "European DEMO design and maintenance strategy", *Fus. Eng. Des.*, 83 (2009), 858-864.

[13] M. Kikuchi, Y. Seki, and K. Nakagawa, "The advanced SSTR", *Fus. Eng. Des.*, 48 (2000), 265-270.

[14] D. Steiner, E. Cheng, R. Miller, "The ARIES-fusion neutron source study", *UCSD-ENG-0083*, August, 2000.

[15] Y.C. Wu, et al., "Conceptual design activities of FDS series fusion power plants in China", *Fus. Eng. Des.*, 81 (2006).

[16] A. Sagara, O. Mitarai, S. Imagawa, et al., "Conceptual design activities and key issues on LHD-type reactor FFHR", *Fus. Eng. Des.*, 81 (2006) 2703-2712.

[17] K Karl Ehrlich, E.E. Bloom, T. Kondo, et al., "International strategy for fusion materials development", *J. Nucl. Mater.* 283-287 (2000) 79-88.

[18] M. Seki, M. Guseva, G. Vieider, et al, *J. Nucl. Mater.* 179-181 (1991) 1189-1192.

[19] T. Muroga, T. Tanaka, S. Sagara, et al., *Fus. Eng. Des.*, 81 (2006) 1203-1209.

[20] D. L. Smith, C. C. Baker, D. K. Sze, et al, *Fus. Tech.* 8 (1985) 10-44.

[21] K. Ehrlich, E.E. Bloom, T. Kondo, et al., *J. Nucl. Mater.* 283-287 (2000) 79-88.

[22] C.P.C. Wong, J.-F. Salavy, Y. Kim, et al., "Overview of liquid metal TBM concepts and programs", *Fus. Eng. Des.*, 83 (2008) 1788-1791.

[23] J.W. Davis, "The role of materials R&D in the development of commercial fusion power plants", *J. Nucl. Mater.*, 271-272 (1999) 532-537

[24] G. Cambi, L. Di Pace, D.G. Cepraga, et al., "Materials optimization for fusion power plants waste management from neutronics and activation assessment", *Fus. Eng. Des.*, 69 (2003) 705-709.

[25] A. Kimura, T. Morimura, M. Narui, et al., "Irradiation hardening of reduced activation martensitic steels", *J. Nucl. Mater.*, 233-237 (1996) 319-325.

[26] N. Yamamotoa, Y. Murase, J. Nagakawa, "An evaluation of helium embrittlement resistance of reduced activation martensitic steels", *Fus. Eng. Des.*, 81 (2006) 1085-1090.

[27] Y. de Carlan, M. Murugananth,T. Sourmail, et al., "Design of new Fe-9CrWV reduced-activation martensitic steels for creep properties at 650°C", *J. Nucl. Mater.*, 329-333 (2004) 238-242.

[28] T. Flament, P. Tortorelli, V. Coen, et al., "Compatibility of materials in fusion first wall and blanket structures cooled by liquid metals", *J. Nucl. Mater.*, 191-194 (1992) 139-145.

[29] J. Konys, W. Krauss, J. Novotny, et al., "Compatibility behavior of EUROFER steel in flowing Pb-17Li", *J.Nucl. Mater.*, 386-388 (2009) 678-681.

[30] J.B. Vogt, A.Verleene, I. Serre, et al., "Understanding the liquid metal assisted damage sources in the T91 martensitic steel for safer use of ADS", *Engineering Failure Analysis*, 14 (2007) 1185-1193.

[31] E.T. Cheng, "Waste management aspect of low activation materials", *Fus. Eng. Des.* 48 (2000) 455-465.

[32] D.L. Smith, H, M, Chung, B. A. Loomis, et al., "Development of vanadium-base alloys for fusion first-wall-blanket applications", *Fus. Eng. Des.* 29 (1995) 399-410.

[33] B.van der Schaaf, K. Ehrlich, P. Fenici, "European structural materials development for fusion applications", *Fus. Eng. Des.* 48 (2000) 499-508.

[34] Y. Seki, T. Tabara, I. Aoki, et al., "Composition adjustment of low activation materials for shallow land burial", *Fus. Eng. Des.* 48 (2000) 435-441.

[35] R.L. Klueh, A.T. Nelson, "Ferritic/martensitic steels for next-generation reactors", *J. Nucl. Mater.*, 371 (2007) 37-52.

[36] D.L. Smith, H.M. Chung, B.A. Loomis, "Development of vanadium-base alloys for fusion first-wall-blanket applications", *Fus. Eng. Des.*, 29 (1995) 399-410.

[37] R.J. Kurtz, K. Abe, V.M. Chernov, "Recent progress on development of vanadium alloys for fusion", *J. Nucl. Mater.*, 329-333 (2004) 47-55.

[38] T. Muroga, T. Nagasaka, K. Abe, et al., "Vanadium alloys - overview and recent results", *J. Nucl. Mater.*, 307-311 (2002) 547-554.

[39] A.K. Shikov, V.A. Beliakov, "Overview of recent Russian materials and technologies R&D activities related to ITER and DEMO constructions", *J. Nucl. Mater.*, 367-370 (2007) 1298-1304.

[40] T. Muroga, T. Nagasaka, A. Iiyoshi, et al., "NIFS program for large ingot production of a V-Cr-Ti alloy", *J. Nucl. Mater.*, 283-287 (2000) 711-715.

[41] J.M. Chen, T. Muroga, S.Y. Qiu, et al., "The development of advanced vanadium alloys for fusion applications", *J. Nucl. Mater.*, 329-333 (2004) 401-405.

[42] L.L. Snead, R.H. Jones, A. Kohyama, et al., "Status of silicon carbide, composites for fusion", *J. Nucl. Mater.*, 233-237 (1996) 26-36.

[43] A.R. Raffray, R. Jones, G. Aiello, et al., "Design and material issues for high performance SiCf/SiC-based fusion power cores", *Fus. Eng. Des.*, 55 (2001) 55-95.

[44] L. Giancarli, H. Golfier, S. Nishio, et al., "Progress in blanket designs using SiCf/SiC composites", *Fus. Eng. Des.*, 61- 62 (2002) 307-318.

[45] L. Giancarli, G. Aiello, A. Caso, et al., "R&D issues for SiC_f/SiC composites structural material in fusion power reactor blankets", *Fus. Eng. Des.*, 48 (2000) 509-520.

[46] K. Shimoda, J.S. Park, T. Hinoki, et al., "Microstructural optimization of high-temperature SiC/SiC composites by NITE process", *J. Nucl. Mater.*, 386-388 (2009) 634-638.

[47] R.H. Jones, H.L. Heinisch, K.A. Mcarthy, et al., "Low activation materials", *J. Nucl. Mater.*, 271-272 (1999) 518-525.

[48] S.N. Rosenwasser et al., "The application of martensitic stainless steels in long lifetime fusion first wall/blankets", *J. Nucl. Mater.*, 85-86 (1979).

[49] R.L. Klueh, J.M. Vitek and M.L. Grossbeck, Proc. 11th Conf. on Effects of Irradiation on Materials, ASTM-STP 782, eds. H.R. Brager and J.S. Perrin (American Society for Testing Materials, Philadelphia, 1982) p. 648.

[50] P. Schiller, "Review of materials selection for fusion reactors", *J. Nucl. Mater.*, 206 (1993) 113-120.

[51] A. Kohyama, A. Hishinuma, D.S. Gelles, et al., "Low-activation ferritic and martensitic steels for fusion application", *J. Nucl. Mater.*, 233-237 (1996) 138-147.

[52] Q. Huang, C. Li, Y. Li, et al., "Progress in development of China Low Activation Martensitic steel for fusion application", *J. Nucl. Mater.*, 367-370 (2007) 142-146.

[53] R.L. Klueh and P.J. Maziasz, "Microstructure of Cr-W steels", *Met. Trans.* 20A (1989) 373-381.

[54] R.L. Klueh, D.S. Gelles, S. Jitsukawa, et al., "Ferritic/martensitic steels- overview of recent results", *J. Nucl. Mater.*, 307-311 (2002) 455-465.

[55]B. van der Schaaf, F. Tavassoli, C. Fazio, et al., "The development of EUROFER reduced activation steel", *Fus. Eng. Des.*, 69 (2003) 197-203.

[56] K.M. Feng, C.H. Pan, G.S. Zhang, et al., "Overview of design and R&D of solid breeder TBM in China", *Fus. Eng. Des.*, 83 (2008) 1149-1156

[57] R.L. Klueh, D.S. Gelles and T.A. lechtenberg, "Development of ferritic steels for reduced activation - the US program", *J. Nucl. Mater.*, 141-143 (1986) 1081-1087.

[58] R.L. Klueh and P.J. Maziasz, *Metall. Trans. A* 20 (1989)

[59] R.L. Klueh and W.R. Corwin, *J. Eng. Mater.* 11 (1989)

[60] W.L. Hu and D.S. Gelles, Proc. 13th Int. Symp. On Influence of Radiation on Material Properties, Part II, ASTM-STP 956, eds. F.A. Garner, C.H. Henager, Jr. and N. Igata (American Society for Testing Materials, Philadelphia, 1987) p. 83.

[61] R.L. Klueh and D.J. Alexander, "Impact toughness of irradiated reduced-activation ferritic steels", *J. Nucl. Mater.* 212-215 (1994) 736.

[62] E.S. Jitsukawa, M. Tamura, B.Schaaf, et al., "Development of an extensive database of mechanical and physical properties for reduced-activation martensitic steel F82H", *J. Nucl. Mater.*, 307-311 (2002) 179-186

[63] K. Shiba, T. Sawai, Y. Kohno, et al., "Report of IEA Workshop on Reduced - Activation Ferritic/Martensitic Steels", *JAERI-Conf.* 2001-007, p. 151.

[64] S. Jitsukawa and K. Shiba, "The reduced activation ferritic/martensitic steel as a structural material for the test blanket modules", *Mater. Assessment Report*, 2000.

[65] A Kohyama, Y. Kohno, K. Asakura, "R&L D of low activation ferritic steels for fusion in Japanese universities", *J. Nucl. Mater.*, 212-215 (1994) 684-689.

[66] A. Kohyama, A. Hishinuma, D. S. Gelles et al., "Low-activation ferritic and martensitic steels for fusion application", *J. Nucl. Mate.,* 233-237 (1996) 138-147.

[67] Y.F. Li, Q. Huang, Y. Wu, et al., "Mechanical properties and microstructures of China low activation martensitic steel compared with JLF-1", *J. Nucl. Mater.*, 367-370 (2007) 117-121.

[68] H.L. Li, A. Nishimura, T. Muroga, et al., "Fatigue life and strain hardening behavior of JLF-1 steel", *J. Nucl. Mater.*, 386-388 (2009) 433-436.

[69] P. Fern´andez, A.M. Lancha, J. Lape˜na, et al., "Creep strength of reduced activation ferritic/martensitic steel Eurofer'97", *Fus. Eng. Des.*,75-79 (2005) 1003-1008.

[70] R. Andreani, M. Gasparotto, "Overview of fusion nuclear technology in Europe", *Fus. Eng. Des.*, 61-62 (2002) 27-36.

[71] J. Yu, Q. Huang, F. Wan, et al., "Research and development on the China low activation martensitic steel (CLAM)", *J. Nucl. Mater.*, 367-370 (2007) 97-101.

[72] Q. Huang, M. Zhang, Z. Zhu, et al., "Corrosion experiment in the first liquid metal LiPb loop of China", *Fus. Eng. Des.*, 82 (2007) 2655-2659.

[73] C. Li, Q. Huang, P. Zhang, et al., "Preliminary experimental study on Hot Isostatic Pressing diffusion bonding for CLAM-CLAM", *Fus. Eng. Des.*, 82 (2007) 2627-2633.

[74] F. Zhao, J. Qiao, Y.Huang, et al., "Effect of irradiation temperature on void swelling of China Low Activation Martensitic steel (CLAM)", *Mater. Chara.*, 59 (2008) 344-347.

[75] A-A.F. Tavassoli, "Present limits and improvements of structural materials for fusion reactors - a review", *J. Nucl. Mater.*, 302 (2002) 73-88.

[76] B. van der Schaaf, D.S. Gelles, S. Jitsukawa, et al., "Progress and critical issues of reduced activation ferritic/martensitic steel development", *J. Nucl. Mater.*, 283-287 (2000) 52-59.

[77] A. Kohyama, Y. Katoh, M. Ando, et al., "A new Multiple Beams-Material Interaction Research Facility for radiation damage studies in fusion materials", *Fus. Eng. Des.*, 51-52 (2000) 789-795.

[78] Brian S. Mitchell, *Mater. Eng. Sci.*, ISBN 0-471-43623-2, 2004 John Wiley & Sons, Inc.

[79] Y. de Carlan, A. Alamo, M,H. Mathon, et al., "Effect of thermal ageing on the microstructure and mechanical properties of 7-11 CrW steels", *J. Nucl. Mater.*, 283-287 (2000) 672-676.

[80] J. Lapeña, M. Garcia-Mazario, P. Fernández, et al., "Chemical segregation behavior under thermal aging of the low-activation F82H-modified steel", *J. Nucl. Mater.*, 283-287 (2000) 662-666.

[81] B.van der Schaaf (Ed.), "Hardening and Toughness from Radiation, and Reference Characterization of F82H and Screening Steels", August 1999, SM milestone 4 report, NRG doc.nr. 25387

[82] R.L. Klueh (Ed.), Proceedings of the IEA Workshop/ Working Group Meeting on Ferritic/Martensitic Steels, Petten NRG, ORNL/M-6627, 1&2 October, 1998.

[83] L. Sch afer, M. Schirra, et al., "Infuence of thermal aging on tensile and impact bending properties of the steel grades OPTIFER and F82H-mod", *J. Nucl. Mater.*, 271-272 (1999) 455-458.

[84] P. Fernandez, A.M. Lancha, J. Lapena, et al., "Metallurgical properties of reduced activation martensitic steel Eurofer97 in the as-received condition and after thermal ageing", *J. Nucl. Mater.*, 307-311 (2002) 495-499.

[85] R. Lindau, A. Moslang, M. Schirra, "Thermal and mechanical behaviour of the reduced-activationferritic-martensitic steel EUROFER", *Fus. Eng. Des.*, 61-62 (2002) 659-664.

[86] M. Rieth, M. Schirra, A. Falkenstein, et al., "Eurofer 97-Tensile, Charpy, Creep and Structural Tests", *FZKA* 6911, 2003.

[87] T. M. Tamura, K. Shinozuka, H. Esaka, et al., "Mechanical properties of 8Cr-2WVTa steel aged for 30 000 h", J. Nucl. Mater., 283-287 (2000) 667-671.

[88] H. Tanigawa, K. Shi., S. Jitsukawa, et al., "Thermal ageing behavior of reduced activation martensitic steel-F82H", presentation in *ICFRM-13*, Nice, France, Dec.9-12, 2007.

[89] R.E. Smallman, R. J. Bishop, *Modern Physical Metallurgy and Materials Engineering*, ISBN 0 7506 4564 4, 1999.

[90] P. Ferna´ndez, A.M. Lancha, J. Lapen˜a, et al., "Metallurgical characterization of the reduced activation ferritic/martensitic steel Eurofer'97 on as-received condition", *Fus. Eng. Des.*, 58-59 (2001) 787-792.

[91] Michael E. Kassner, Mari'a-Teresa Pe'rez-Prado, "Fundamentals of Creep in Metals and Alloys", ISBN: 0-08-043637-4, 2004.

[92] Josef Betten, "Creep mechacnics", New York, ISBN 3-540-23204-4, 2005.

[93] R.W. Evans, J.A. Preston, B. Wilshire, et al., "Creep and creep fracture of an oxide-dispersion-strengthened 13% chromium ferritic steel", *Mater. Sci. Eng: A*, 19 (1993) 65-72.

[94] B. Wilshire, M.T. Whittaker, "The role of grain boundaries in creep strain accumulation", *Acta Mater.*, (2009), doi:10.1016/j.actamat.2009.05.009.

[95] E. Cerri, E. Evangelista, S. Spigarelli, et al., "Evolution of microstructure in a modified 9Cr-1Mo steel during short term creep", *Mater. Sci. Eng. A,* 245 (1998) 285-292.

[96] F. Abe, S. Nakazawa, *Metall. Trans.* 23A (1992) 3025.

[97] A. Alamo, V. Lambard, X. Averty, et al., "Assessment of ODS-14%Cr ferritic alloy for high temperature applications", *J. Nucl. Mater.*, 29-333 (2004) 333-337.

[98] A.L. Bement, et al., "Fundamental Materials Problem in Nuclear Rectors," *Proc. 2nd International Conference on The Strength of Metals and Alloys*, ASM, Metals Park, OH, 693, (1970).

[99] F.A. Garner, M.L. Hamilton, N.F. Panayotou, et al., "The microstructure origins of yield strength changes in AISI 316 during fission or fusion irradiation," *J. Nucl. Mater.,* 103-104, 803 (1981).

[100] T. Muroga, K. Yasunaga, Y. Katoh, et al., "Correlation of hardening and Microstructure of Tantalum Irradiated with Heavy Ions," *American Society for Testing and Materials*, 100 Barr

Harbor Drive, West Conshohocken, 2959 (2000).

[101] D. Tabor, *The hardness of Metals*, Oxford University Press, Oxford, UK, (1951).

[102] A. D. McNaught and A. Wilkinson, *Compendium of Chemical Terminology,* Second Edition, Blackwell Science, ISBN 0865426848, 1997.

[103] N. Igata, H.B. Chen and K. Miyahara, "An internal friction peak due to stress induced a' martensite in a SUS304 steel", *Journal De Physique*, 43 (1982) 547.

[104] S. Raju, B. Ganesh, A. Banerjee, et al., "Phase Stability Characterization and Thermodynamic Data Generation on 9Cr-1Mo Steel with varied Microstructure-Based on Experimental Measurements and Modeling", *Mater. Sci. Eng., A* 465 (2007) 29.

[105] J. Hald, "Microstructure and long-term creep properties of 9-12%Cr steel", *Int. J. Pressure Vessels and Piping,* 85 (2008) 30-37.

[106] F. Abe, "Creep rates and strengthening mechanisms in tungsten-strengthened 9Cr steels," *Mater. Sci. Eng. A*, 319-321 (2001) 770.

[107] F. Abe, "Bainitic and martensitic creep resistant steels," *Current Opinion in Solid State and Materials Science*, 8 (2004) 305.

[108] V. Sklenicka, K. Kucharova, M. Svoboda, et al., "Long-term creep behavior of 9-12%Cr power plant steels," *Mater Character*, 51 (2003) 35.

[109] H. Kushima, K. Kishima and F. Abe, "Degradation of 9Cr-1Mo steel during long-term creep deformation," *Testu-to-Hagane,* 85 (1999) 841.

[110] A. Iseda, H. Teranihsi and F. Masuyama, "Effect of chemical compositions and heat treatments on creep rupture strength of 12%Cr heat resistant steels for boiler," *Testu-to-Hagane,* 76 (1990) 1076

[111] M. Tamura, H. Kusuyama, K. Shinozuka, et al., "Long-term stability of TaC particles during tempering of 8%Cr-2%W steel," *J. Nucl. Mater.,* 367-370 (2007) 137.

[112] P. Fernández, A.M. Lancha, J. Lapeña, et al., "Metallurgical properties of reduced activation martensitic steel - Eurofer 97 in the as-received condition and after thermal aging." *J. Nucl. Mater.,* 307-311 (2002) 495.

[113] M. Tamura, K. Ikeda, H. Esaka, et al., *ISIJ INT.,* 41 (2001) 908.

[114] N.J. Petch, *J. Iron Steel. Inst.*, 173 (1953) 25-28.

[115] T. Nagasaka, H. Yoshida, K. Fukumoto, et al., "Mechanical properties of a high-purity Fe-9Cr-2W-0.1C model alloy for low-activation ferritic steels for fusion reactors", *Mater.Trans. JIM*, 41 (2000) 170-177.

[116] J.P. Naylor, *Metall. Trans.,10A* (1979), 861-873.

[117] M. Klesnil, M. Holzmann, P. Lukas and P. Rys, *J. Iron and Steel.Inst.,* (1965) 47-53.

[118] R.L. Klueh, D.J. Alexander, "Effect of heat treatment and irradiation temperature on impact properties of Cr-W-V ferritic steels", *J. Nucl.Mater.*, 265 (1999) 262-272.

[119] H. Kayano, A. Kimura, M. Narui, et l., *J. Nucl.Mater.*155-157 (1988) 978.

[120] R.L. Klueh, D.J. Alexander, M.A. Sokolov, et al., "Effect of chromium, tungsten, tantalum, and boron on mechanical properties of 5-9Cr-WVTaB steels", *J. Nucl. Mater.*,304 (2002) 139-152.

[121] A. Alamo, J. C. Brachet, A. Castaing, et al., "Physical metallurgy and mechanical behaviour of FeCrWTaV low activation martensitic steels: Effects of chemical composition", *J. Nucl. Mater.*, 258-263 (1998) 1228-1235.

[122] C. Petersen, and H. Tanigawa et al., 21th IAEA Fusion Energy Conference, Chengdu, Oct.18, 2006.

[123] F.C. Monkman, *N.J. Grant, Proc ASTM*, 56 (1956) 593.

[124] F.R. Larson and James Miller, *Trans. ASTM,* 74 (1952) 765.

[125] G. Dimmler, P. Weinert, and H. Cerjak, *Int. J. Press. Vess. Pip.*, 85 (2008) 55.

[126] P. Fernández, A.M. Lancha, J. Lapeña, et al., *Fus. Eng. & Des.* 75-79 (2005) 1003.

[127] M. Tamura, et al., *ISIJ International*, 39 (1999) 380-387.

LISTS OF PUBLICATION PAPERS

1. **Y.F. Li**, T. Nagasaka, T. Muroga, Q.Y. Huang and Y.C. Wu, "Effect of thermal ageing on tensile and creep properties of JLF-1 and CLAM steels", *J. Nucl. Mater.*386-388 (2009) 495-498.

2. **Yanfen Li**, T. Nagasaka, T. Muroga, "Creep properties and microstructure of JLF-1 and CLAM steels aged at 823 to 973 K", *Fusion Sci. and Tech.*, 56 (2009) 323-327.

3. **Yanfen Li**, T. Nagasaka, T. Muroga, "Ageing effects on tensile properties of JLF-1 and CLAM steels", *NIFS proceeding*, Page:104-109, 2009.

4. **Yanfen Li**, T. Nagasaka, T. Muroga, "Long-term thermal stability of reduced activation ferritic/martensitic steels as structural materials of fusion blanket", *Plasma and Fusion Research,* (accepted for publication), 2009.

5. **Yanfen Li**, T. Nagasaka, T. Muroga, "Influence of Stress during Thermal Ageing on Microstructure and Mechanical properties on JLF-1 and CLAM steels", submitted to the 14th International Conference of Fusion Reactor Material- ICFRM-14, Sapporo, Japan, Sep. 6-11, 2009.

LISTS OF PRESENTATIONS

1. **Yanfen Li**, T. Nagasaka, T. Muroga, Q. Y. Huang, Y.C. Wu, Effects of thermal ageing on tensile and creep properties of JLF-1 and CLAM steels, *13th International Conference of Fusion Reactor Materials (ICFRM-13)*, Nice, France, Dec.10-14, 2007.

2. **Yanfen Li**, T. Nagasaka, T. Muroga, Effects of thermal ageing on tensile and creep properties of JLF-1 steels, *Autumn Meeting of the Japan Institutes of Metals*, Gifu, Japan, Sep.19-21, 2007.

3. **Yanfen Li**, T. Nagasaka, T. Muroga, Creep properties and microstructure of JLF-1 and CLAM steels aged at 823 to 973 K, *18th Totic of Fusion Energy,* San Francisco, USA, Sep. 28 to Oct. 2, 2008.

4. **Yanfen Li,** T. Nagasaka, T. Muroga, Ageing effects on tensile properties of JLF-1 and CLAM steels, *China-Japan CUP-CAS on PWI/PFC and Fusion Technologies,* Huangshan, China, Oct.27 - 29, 2008.

5. **Yanfen Li,** T. Nagasaka, T. Muroga, Long-term thermal stability of reduced activation ferritic/martensitic steels as structural materials of fusion blanket, *18th International Toki Conference,* Toki, Japan, Dec. 9-12, 2008.

6. **Yanfen Li,** T. Nagasaka, T. Muroga, Thermal ageing and creep behavior of JLF-1 and CLAM steels, *Spring Meeting of the Japan Institutes of Metals*, Tokyo, Japan, Mar. 28-30, 2009.

7. **Yanfen Li,** T. Nagasaka, T. Muroga, Influence of Stress during Thermal Ageing on Microstructure and Mechanical properties on JLF-1 and CLAM steels, *14th International Conference of Fusion Reactor Material*, Sapporo, Japan, Sep. 6-11, 2009.

ACKNOWLEDGE

Firstly, I would like to express my great appreciation to supervisor – Prof. Takeo MUROGA in National Institute for Fusion Science (NIFS) and the Graduate University for Advanced Studies (SOKENDAI). I very appreciated him to give me the good chance to study in Japan. Professor helped me to propose the main research idea, taught me during all the study period, and guided me to complete this thesis paper.

Also I would like to give great thanks to my assistant supervisor – Associate Prof. Takuya NAGASAKA in NIFS. He supported me during the experiments, and gave me much help and guidance for study and living in Japan.

This work was supported by NIFS Budget Code NIFS07UCFF003 and NIFS07GCFF003, and also supported by JSPS-CAS Core University Program.

The CLAM steel was prepared in Institute Plasma Physics, Chinese Academy Sciences (ASIPP) in the cooperation with Institute of Metal Research, Chinese Academy Sciences (ASIMR). Much thanks to Prof. Yican WU and Prof. Qunying HUANG in Fusion Design Study (FDS) division in ASIPP for supporting me to study in Japan and their guidance. Thanks also to Prof. Yiyin SAN et al. in ASIMR to prepare the CLAM steel.

I further express my thanks to Professors NODA, SAGARA and NISHIMURA in Fusion Engineering Research Center (FEC) in NIFS for their guided comments. I also extend thanks to Dr. HISHINUMA, Dr. TANAKA, Dr. KONDO, and other members in our center for their aids and collaborations on this study.

I want to thank my good friends, Zaixin LI, Qi XU and Dongxun ZHANG, et al., for their helps and encouragement in study and daily life in Japan.

Finally, I would like to express the best appreciations to my family (father - Yousheng LI, mother - Ruiying SUN, and sister - Yanchun-LI) and husband (Chunlin CHEN). Their love and support are the spiritual source for me to finish this research and the thesis successfully.

Yanfen LI

Sep. 20, 2009